1974

Frame Transformations in Electron-Molecule Scattering.

Charles Albert Weatherford
Louisiana State University and Agricultural & Mechanical College

Frame Transformations in Electron-Molecule Scattering

A Dissertation

Submitted to the Graduate Faculty of the
Louisiana State University and
Agricultural and Mechanical College
in partial fulfillment of the
requirements for the degree of
Doctor of Philosophy

in

The Department of Physics and Astronomy

by
Charles Albert Weatherford
B.S., Louisiana State University, 1969
August, 1974

ACKNOWLEDGEMENTS

The assistance, encouragement and patience of Dr. R. J. W. Henry throughout the course of this work was of great value and I offer my sincere gratitude. In addition, I wish to thank Dr. E. R. Smith, Dr. S. P. Rountree, and Dr. B. Tambe for their valuable technical assistance.

The author acknowledges the financial support of the Department of Physics and Astronomy, the National Science Foundation, and the Charles E. Coates Memorial Fund. The author is also indebted to the Computer Research Center for the use of their facilities.

Finally, the author dedicates this thesis to his parents.

TABLE OF CONTENTS

LIST OF TABLES

LIST OF FIGURES

ABSTRACT

The noniterative integral equation technique is used to solve the linear, ordinary, second-order coupled differential equations that result from a treatment of the electron-molecule scattering problem within the close-coupling theory. In order to compensate for truncation of the close-coupling system wavefunction expansion, alternative coordinate reference frames (lab and body) are used to describe the incident electron trajectory. The transformation between the two frames, within the framework of the integral equation quadrature, is described and then applied to the scattering problem to calculate pure rotational cross sections, $\sigma(\Delta v=0, \Delta j=2)$, pure vibrational cross sections, $\sigma(v=0\rightarrow 1, \Delta j=0)$ and simultaneous rotational-vibrational cross sections, $\sigma(v=0\rightarrow 1, \Delta j=2)$. In the results of calculation, support for experimentally observed structures, believed to be rotational resonances, is evident.

CHAPTER I

INTRODUCTION

A. Motivation for the Physical Model

Quantum mechanics (QM) is accepted by most physicists and chemists to be the correct description of the dynamics of atomic and molecular systems. The time-independent, coordinate-space form of Schroedinger's equation (TICSSE) is regarded, by atomic and molecular physicsts, and chemists, as the most straight-forwardly applied approach. Perhaps this is so because there are immediately available rules for writing down the equation in a form general enough to apply to all atomic and molecular systems; one of course assumes that the system is composed of particles moving under the influence of electromagnetic forces. The problem that is immediately encountered is the generation of a solution for any potential. The equation is a second order, linear, partial differential equation: the only hope for exact solution lies in a separation of variables. We quickly find that this can be done exactly only when we are able to define the variables with respect to a co-ordinate system that reduces the resulting equations to single variable equations. Only one atomic system yields to such an exact treatment: the hydrogen atom.

The motivation for choosing the TICSSE approach to QM is the desire to find a generally applicable recipe for

obtaining quantitative information about electromagnetic systems. Consistent with this motivation, one attempts to apply the procedure which furnishes the exact solution to the hydrogenic system, to more complicated systems. This procedure applied to atomic systems takes the form of the Central-Field Approximation (CFA).[1] In the CFA, each electron is described by a hydrogenic orbital

$$\psi_k(n\ell m_\ell) = r^{-1} R_{n\ell}(r) Y_{\ell m_\ell}(\theta,\phi) \qquad (1.1)$$

where the $Y_{\ell m_\ell}$ are spherical harmonics and the $R_{n\ell}$ are called Slater Orbitals (SO);

$$R_{n\ell}(r) = \sum_{i=1}^{n-\ell} C_i r^{n_i} e^{-\alpha_i r} \qquad (1.2)$$

Atomic wave functions are then formed from determinants composed of the one-electron orbitals. The α_i's are determined by forming the Hamiltonian matrix elements

$$H_{ik}^{LS\pi} = \langle \psi_i | \hat{H}_N | \psi_k \rangle^{LS\pi} \qquad (1.3)$$

(we have restricted our description to the LSπ coupling scheme) and varying α_i in (1.2) to minimize the eigenvalues obtained by diagonalizing the Hamiltonian matrix. The angular part of the atomic wave function is determined by specifying the total system orbital angular momentum,

spin, and parity ($LS\pi$), and then coupling the individual angular parts of the SO's to give the overall $LS\pi$ desired. Now for a given $LS\pi$, there is in general more than one way to place the electrons in the orbitals and couple them. To account for this, each atomic wave function $\phi^{LS\pi}$ is expanded as a sum over all possible ways to compose the state; this is called a configuration expansion. The point to be made concerns the central assumption of the CFA; namely that the interaction potential,

$$V_{ij} = -\sum_{i=1}^{N} \frac{Ze^2}{r_i} + \sum_{i>j}^{N} \frac{e^2}{r_{ij}}$$

e charge per electron

Z number of positive charges of magnitude e in the nucleus

N total number of electrons

r_i distance of electron i from nucleus

r_{ij} distance of electron i from electron j

(1.4)

is a perturbation on some spherically symmetric potential $U(r_i)$ describing the screening effect of all electrons in closed shells. Thus we see that the success of the CFA lies in the validity of this assumption. Also the whole concept of forming atomic system wave functions from one

electron orbitals depends on this assumption for its validity.

Having at least qualitatively isolated the critical test of the CFA, which is the application of the TICSSE approach to atomic bound state systems, and observed its extensively documented success, we proceed to push the method as far as it is applicable. Immediately we are faced with a universe of atoms quantum mechanically bound into molecules. We again wish to use an approach that is straight-forwardly applicable to any molecular system. Our objective is of course to obtain molecular system wave functions sufficiently accurate to provide reliable predictions of physically observable molecular quantities. We now face the problem of multiple nuclei. Because of mass differences the system wave function will naturally decouple into a product of a nuclear function times an electronic function: this is the physical content of the Born-Oppenheimer Approximation (BOA).

Consistent with the model outlined above, the molecular electronic wave function is composed of one electron Slater-type orbitals. The problem is to decide how to combine these orbitals. Essentially three conditions must be considered[2]; (1) the orbitals must overlap, (2) the orbitals must have matching energy, (3) the orbitals must be coupled to give the correct geometrical symmetry of the molecular state considered. The most successful

technique is the LCAO-MO-SCF (linear combination of atomic orbitals - molecular orbital - self-consistent field). The molecular wave function is expanded in a basis of Slater orbitals about each of the nuclei. In order to simplify the resulting integrals the Slater orbitals are in turn expanded about a common center of coordinates located at the center of mass of the molecule.

The degrees of freedom of the nuclei are described by the rotational and vibrational quantum numbers. The vibrational and rotational motion are assumed to be uncoupled. The rotational motion is described by the equations of a rigid rotator and the vibrational motion by a harmonic oscillator.

Thus is outlined an approach to a description of molecular systems. The description is assumed sufficiently accurate to describe the molecule as it participates in a physical process. One process of interest is electron-molecule collision: obviously a time-dependent process. The physical setting in which this process usually occurs is a continuous beam of non-interacting electrons passing through a sufficiently pressureless gas so that the molecules are effectively isolated and thus non-interacting. Then the process may abstractly be visualized as an infinite ensemble of single collisions between an electron and molecule. Consistent with the TICSSE approach, the process is assumed to be described by a time-

independent Schroedinger equation. It is thus obvious that there are possibly severe approximations involved here. Accepting this, in lieu of a more realistic yet equally tractible method, the model may be applied, as is done in electron-atom collisions, within the framework of close-coupling theory. In short, the attitude taken is to apply the most tractable procedure as realistically as possible to obtain quantitative information about a physically interesting process: electron molecule scattering.

Close-coupling procedures begin with the expansion of the system (target plus projectile) wave function as a product of target states and projectile states describing the projectile as a function of its position with respect to the target when the target is in each of its various possible states. In practice the expansion is truncated and thus only a few of the lowest target states are included in the close-coupling expansion.[3] The projectile states are then described by a set of coupled, second-order, ordinary integro-differential equations with prescribed boundary conditions. The integral part of the equations results from the anti-symmetrization of the total wave function, which is the mathematical consequence of electron exchange. There occurs in the equations, a set of potentials that describe the electron target interaction as a function of the electron position. It is in

the description of the interaction potential that we must face a fundamental difference between the electron-atom collision problem and the electron-molecule collision problem. The coordinate system, as we have described it, is in both cases fixed at the center of mass. In the atomic problem, the only degrees of freedom left are electronic. However, in the molecule problem, both nuclear and electronic degrees of freedom remain.

The potential must, for electron-molecule collisions, realistically describe, in a time-independent manner, the time-dependent interaction of the electron with three different degrees of target state freedom; electronic, nuclear rotation, nuclear vibration. Inherent in the time-independent treatment of the collision is the assumption of the adiabaticity of the process. This implies that the electron configuration, as well as the nuclear configuration, is essentially frozen throughout the encounter. To relax this restriction, a polarization potential is used to describe the dynamic affect of the projectile on the target electron configuration. The adiabatic assumption is less stringent when applied to nuclear motion because of the greater periods of nuclear motion. However, it is still quite a severe restriction for portions of the projectile trajectory. It is this partial adiabaticity of the nuclear motion with respect to the projectile motion that this paper hopes to deal with in a

more realistic manner than has heretofore been done.

The technique used may be described as follows: during the portion of electron-molecule encounter in which the electron is far from the molecule and moving slowly, the period of nuclear motion is assumed to be zero; during the portion of electron-molecule encounter in which the electron is near the molecule and moving fast, the period of nuclear motion is assumed to be infinite. These two assumptions are implemented by describing the collision with respect to two different coordinate frames, the laboratory frame and the body frame. As the electron begins the encounter and is far from the molecule the lab frame is appropriate. At a certain point of its trajectory, the description is changed by switching reference frames to the body frame. In the lab frame, the coordinate system is fixed in space. The body frame coordinate system is attached to the molecule. It is hoped that this frame transformation will resolve the problem of finite nuclear relaxation time sufficiently well to produce more physically realistic results. If the approach is successful, we will have a procedure for straight-forward application to electron encounters with a whole class of small to medium size molecules.

B. Physical Interest of the e^--H_2 Collision

As was pointed out above, the stationary states of a molecule describe three different classes of bounded particle motion: electronic, nuclear rotation, and nuclear vibration. As a consequence, radiation impingent on a molecule may interact with the three classes of bounded motion in different ways, as it indeed does. The consequence of such interaction is the emission or absorption spectra characteristic of each molecule. Electromagnetic interactions are visualized as occurring through multipole moment processes. The charge distribution is pictured as a superposition of charge configurations representing various symmetries of charge separation: dipole configuration, quadrapole configuration, etc. When radiation occurs, it is pictured as a superposition of dipole, quadrapole, etc., wave fronts. Spherically symmetric atoms in an external electric field radiate predominately in the dipole mode because of the strong dipole-like charge separation that exists. In neutral homonuclear molecules, the lowest order moment is the quadrapole moment. Thus unless the molecule is ionic or heteronuclear, there is no dipole radiation. However, for molecules there is also a quite different types of phenomenon called the Raman effect.[4] The Raman effect results from the changing polarizability of a molecule due

to its rotational and vibrational motion. In atoms, the polarizability is a constant and there is no Raman effect. Although the Raman effect, in the strictest sense, applies only the photon-molecule scattering, the same rotational-vibrational selection rules apply to any charged particle collision with a molecule.

The collision induced emission spectrum can best be studied when there is no superimposed multipole moment radiation spectrum, such as is the case for the hydrogen molecule, H_2. One has to deal with a vibrational selection rule $\Delta v=\pm 1$, and a unique rotational selection rule for homonuclear diatomic molecules, $\Delta j=0,\pm 2$. This latter selection rule is contrasted with the dipole selection rule $\Delta j=0,\pm 1$. In addition, the large rotational level spacing in H_2 permits experimental beam measurements[5] of both rotational and vibrational cross sections, thus giving experimental tests of the theoretical model. Molecular hydrogen gas would be thought, at first glance, to be quite abundant since it is very stable at low temperatures. However, the dissociation energy from the ground state, of approximately 4.4763 eV, is much less than the ionization energy of the hydrogen atom. As a result, ultraviolet photons that won't ionize hydrogen atoms, will dissociate H_2.

Nevertheless, the availability of experimental data makes the theoretical quantitative study of rotational and

vibrational excitation processes very attractive. Most experiments done on H_2 are under conditions of thermal equilibrium. Therefore the statistical population of the various rotational and vibrational levels is governed by the Maxwell-Boltzman distribution law. Accordingly, the number of molecules in the vibrational state v is

$$N_v = \frac{N}{Q_v} \exp[-G_o(v)hc/(kT)]$$

$$Q_v = 1 + \sum_{v=1}^{\infty} \exp[-G_o(v)hc/(kT)]$$

n = total number of molecules

h = $4.1354 * 10^{-15}$ (eV)(s)

C = $2.997930 * 10^{10}$ (cm)(s^{-1})

k = $8.6164 * 10^{-5}$ (eV)($°K^{-1}$)

T = temperature in degrees Kelvin

$G_o(v) = \nu_o v$

where

$\nu_o hc = 0.544906$(eV) for H_2

and

v = vibrational quantum number (1.5)

The number of molecules in rotational state j is[4]

$$N_j = \frac{N}{Q_r} (2j+1) \exp[-Bj(j+1)hc/(kT)]$$

$$Q_r = 1 + \sum_{j=1}^{\infty} (2j+1) \exp[-Bj(j+1)hc/(kT)] \qquad (1.6a)$$

where, for H_2,

$$Bhc = 0.00753888\,(eV) \qquad (1.6b)$$

We thus obtain for H_2 at 300°K

$$\{N_v/N\}_{v=0}^{v=2} \sim \{\sim 1.0,\ .7*10^{-10},\ 0\}$$

$$\{Nj/N\}_{j=0}^{j=4} \sim \{.2644857,\ .4427930,\ .2298287,\ .0559196,\ .0069730\} \qquad (1.7)$$

Certainly then, only the first vibrational level and the first three rotational levels need to be considered for thermal energy ($\lesssim$10 eV) e^--H_2 collisions, as ground states.

With this statistical restriction we have then defined a physically interesting collision problem which may be compared directly with experimental data. The problem then is; a 0-10 eV electron collision with H_2 in its ground electronic state with calculations of cross sections for transitions of H_2 between the first two vibrational states and the first four rotational states.

C. History of the e^--H_2 Collision Problem

Henry gives a review of some early work on the e^--H_2 problem[6] and it won't be repeated here. The first attempt to set up an internally consistent model seems to date from Arthurs and Dalgarno's scattering formalism[7] for charged particle, rigid rotator scattering in the framework of close-coupling theory. Another significant step occurred when Ardill and Davidson[8] extended the formalism of Arthurs and Dalgarno to include electron exchange effects within the close-coupling formalism. Then in 1968, Lane and Henry[9] investigated the effect of the polarization of the H_2 ground state electronic configuration, $^1\Sigma_g^+$, on the rotational excitation cross sections with exchange effects included.

In 1970, Henry[6] extended the previous work to include vibrational excitation. He considered the pure vibrational transitions ($v=0\rightarrow1$, $\Delta j=0$) and ($v=0\rightarrow2$, $\Delta j=0$), and the simultaneous rotational-vibrational transition ($v=0\rightarrow1$, $\Delta j=2$) resulting from low energy (0→10 eV)e^--H_2 collisions. Henry found his results to be in generally good agreement with the experimental results of Linder[5]; however, for $2<E<5$ eV, ($v=0\rightarrow1$, $\Delta j=0$) and ($v=0\rightarrow1$, $j=1\rightarrow3$) are 50% larger than experiment. Also, for $E>3$ eV, $\sigma(v=0\rightarrow2, \Delta j=0)$ is underestimated. We note that all the results described so far were obtained using a laboratory

frame of reference.

In a review article,[10] the fixed nuclei approximation is described by Gerjuoy. However, no extensive calculation of excitation cross-sections is reported. Then in 1972, Chang and Fano[11] describe analytically the relationship between the alternative fixed nuclei (body frame) and lab frame approach to electron-molecule collisions. As they describe the relationship, the treatments differ only in that they result from alternative expansions of the total wave function in states described by alternative sets of incompatible quantum numbers. The relationship is analytically represented by a unitary transformation between the alternative expansion functions.

Henry and Chang[12] calculated rotational-vibrational excitation cross-sections by integrating the body frame equations to infinity and then utilizing the frame transformation to obtain the physically meaningful cross-sections. It is at this point that we begin.

Because of the necessity for truncation of the close-coupling expansion, neither the lab frame or the body frame are correct. However, when the electron is far from the molecule, the lab frame is more correct than the body frame. Similarly, near the molecule, the body frame is more correct than the lab frame. What has been done in this work is to partition the electron trajectory between the lab frame and the body frame. Depending on the

particular partial wave and electron energy under consideration, the transformation point may change. The effects of moving the transformation point from zero (lab frame) to infinity (body frame) are studied with exchange included in all cases. The necessity of including exchange to derive realistic results is well known. As is also known, the inclusion of exchange effects complicates the numerical procedure by coupling the value of the projectile scattering function at any particular point "r", to every other point r: $0 \rightarrow \infty$. In setting up a numerical procedure to perform the "dynamic" frame t-ansformation, it would be desirable to noniteratively begin the integration procedure at r=0 in the body frame with exchange included; continue the integration to the transformation point, r_t; perform the transformation and continue integration to $r=\infty$ in the lab frame and then calculate the cross sections from the resulting lab frame R-matrix elements. This procedure is carried out in this paper for e^--H_2 scattering. The numerical procedure used is the noniterative, integral equation quadrature of the close-coupling integrodifferential equations.

The success of the physical model defined above as TICSSE is well documented. Experimental results have been duplicated quite well in shape, and although not as well in magnitude, it is assumed that the sources of error are known. In 1968 L. Frommhold[13] reported structures in the

e^--H_2 scattering cross section below 100 meV. He suggested several possible physical explanations, among them, density dependent dimer effects, electronic resonance trapping, and rotational resonance trapping. Then in 1972, Raith and Land[15] reported similar structures at much lower H_2 density. From this it is inferred that the trapping mechanism is a single e^--H_2 interaction and involves no dimer effects. Further, from the energy location of the structures, they appear to be associated with rotational trapping effects. If the last conclusion is true, the theoretical verification of the rotational resonances might be a critical validation of the TICSSE approach to electron molecule scattering using single-center molecular wave functions.

The rest of the paper is organized as follows: a discussion of molecular bound-state wave functions with particular emphasis on homonuclear diatomic molecules is given in Chapter II; in Chapter III, the alternative laboratory and body frame formulations of the e^--H_2 close-coupling equations are discussed; Chapter IV proceeds to define the unitary transformation between the lab and body frames including a discussion of the conditions for the validity of each; in Chapter V, the noniterative integral equation formulation (NIIEM) of the close-coupling equations is briefly reviewed and is applied to the frame transformation equations; finally, the frame transformation

results are presented in Chapter VI. A set of appendices are also included: Appendix A discusses the polarization potential used in the frame transformation; Appendix B discusses the extension of the procedure to non-neutral systems.

CHAPTER II

MOLECULAR BOUND STATE

A. Born-Oppenheimer Approximation

The types of internal motion of a molecule may be classified into electronic, nuclear rotation, and nuclear vibration. Thus we immediately are faced with a situation much more complex than for atoms. In addition, the field is no longer spherically symmetric.[15] The single simplifying feature, first recognized by Born and Oppenheimer,[16] is the large mass difference between nucleons and electrons. The significance lies in the resulting difference in the kinetic energy of the nuclei, E_N, and the kinetic energy of the electrons, E_e. The kinetic energy of the electrons is much greater than the kinetic energy of the nuclei and thus the period of electronic motion is much shorter. It can be shown[15] using the uncertainty principle that $E_e \sim 2$ eV, $E_v \sim .1$ eV, where E_v is a typical vibrational energy level separation, and $E_r \sim .001$ eV, where E_r is a typical rotational energy level separation. The period of motion is on the order of $\hbar$ divided by the energy; so indeed, the electronic period is at least an order of magnitude less than a typical nuclear period. The effect is that the nuclei may be considered to be fixed when calculating electronic energy levels. Thus, electronic energies depend

parametrically on the positions of the nuclei; instead of getting a single number defining the energy of an electronic state, we in general get a multidimensional surface representing the continuous change of the electronic energy as the orientation of the nuclei change. For the special case of a diatomic molecule, the energy is given by a one dimensional energy curve defined as a function of the internuclear separation "s" (see Fig. 1).

The TICSSE equation, for a molecule, is in atomic units

$$\left[-\sum_{i=1}^{N_e}\frac{\nabla_i^2}{2}-\sum_{j=1}^{N_n}\frac{1}{u_j}\frac{\nabla_j^2}{2}+V(\{\vec{S}_p\}_{p=1}^{N_n};\{\vec{r}_p\}_{p=1}^{N_e})-E\right]$$

$$*\,\Psi(\{\vec{S}_p\}_{p=1}^{N_n};\{\vec{r}_p\}_{p=1}^{N_e})=0$$

where

N_n = number of nuclei in the molecule
N_e = number of electrons in the molecule
u_j = reduced mass of the j'th nucleus
$\vec{S}_p$ = position vector of the p'th nucleus
$\vec{r}_p$ = position vector of the p'th electron
E = total energy of the molecule (2.1)

Based on the relative smallness of the kinetic energy of the nuclei, we invoke the Born-Oppenheimer approximation and neglect it. Thus

$$\Psi(\{\vec{S}_p\}\ ,\ \{\vec{r}_p\}) \sim U_{\{\vec{S}_p\}}(\{\vec{r}_p\})\omega(\{\vec{S}_p\}) \qquad (2.2)$$

Thus we define the functions U and ω. Substituting (2.2) into (2.1) gives

$$[-\sum_i \frac{\nabla_i^2}{2} + V(\{\vec{S}_p\}\ ,\ \{\vec{r}_p\})]\ U_{\{\vec{S}_p\}}(\{\vec{r}_p\}) = U(\{\vec{S}_p\})$$

$$U_{\{\vec{S}_p\}}(\{\vec{r}_p\}) \qquad (2.3)$$

Note that $U(\{\vec{S}_p\})$ represents a set of eigenvalues. Thus we see[15] that for each set $\{S_p\}_{p=1}^{N_n}$, there is a corresponding electron probability distribution $|U(\{\vec{r}_p\})|^2$. Putting the kinetic energy of the nuclei back into Eq. (2.1) and again substituting (2.2) into (2.1) and using (2.3), we obtain

$$U(\{\vec{r}_p\})\ [-\sum_j \frac{1}{u_j}\frac{\nabla_j^2}{2} + U(\{\vec{S}_p\})-E]\ \omega(\{\vec{S}_p\})$$

$$= \sum_j \frac{1}{2u_j}\ [\omega(\{\vec{S}_p\})\nabla_j^2\ U_{\{\vec{S}_p\}}(\{\vec{r}_p\}) + 2(\nabla_j\omega(\{\vec{S}_p\}))$$

$$*\ (\nabla_j U_{\{\vec{S}_p\}}(\{\vec{r}_p\}))] \qquad (2.4)$$

Projecting $U_{\{\vec{S}_p\}}(\{\vec{r}_p\})$ onto (2.4) and integrating over the N_e dimensional volume space, $\{d\vec{\tau}_p\}_{p=1}^{N_e}$, we obtain

$$\left[-\sum_{j=1}^{N_n} \frac{1}{u_j} \frac{\nabla_j^2}{2} + U(\{\vec{S}_p\}) + W(\{\vec{S}_p\})\right] \omega(\{\vec{S}_p\})$$

$$= E\omega(\{\vec{S}_p\}) \qquad (2.5)$$

where

$$W(\{\vec{S}_p\}) = \sum_{j=1}^{N_n} \frac{1}{2u_j} \int \{d\vec{\tau}\} \left[\nabla_j U_{\{\vec{S}_p\}}(\{\vec{r}_p\})\right]^2 \qquad (2.6)$$

In practice for low rotational and vibrational states, (2.6) is neglected. Also, the process of projecting out the electronic states from the coupled equations (2.4) for the nuclear motion, is not obviously valid. Born and Oppenheimer[16] have shown that this procedure is approximately valid for bound-state calculations in which high vibrational and rotational states are not included.

At this juncture, we wish to point out a possible complication involving Born-Oppenheimer approximated nuclear wave functions, used for target states in a scattering calculation. In the extension to scattering processes, the additional assumption is made that the electronic and nuclear vibrational excitation and relaxation processes are uncoupled; e.g. that the electron cloud dynamically adjusts to the projectile position independent of the nuclear vibration and, in addition, the vibrational excitation and relaxation are independent of the dynamically

adjusting electron configuration. The validity of this additional assumption needs investigation.

B. Symmetries for Homonuclear Diatomic Molecules

Using the Born-Oppenheimer approximation (BOA) we see that the total system wave function factors[15] as

$$\Psi = U_{el}\, \chi_{el}\, U_N\, \chi_N \qquad (2.7)$$

where U_{el} is the electronic spatial function, χ_{el} is the electronic spin function, U_N is the nuclear spatial function, and χ_N is the nuclear spin function. Immediately we make the classification that Ψ is symmetric (antisymmetric) under the interchange of the nuclei if the spin of the nucleus is integral (half-integral). For the case under consideration (homonuclear diatomics), the Hamiltonian is invariant with respect to a reflection in a plane perpendicular to the internuclear axis and passing through the midpoint. Thus U_{el} is either symmetric (g for gerade) or antisymmetric (u for ungerade) under interchange of the two nuclei. In most molecular ground states, U_{el} is symmetric under nuclear reflection; this is the case for H_2.

Thus for U_{el} symmetric with respect to nuclear interchange, $U_N\chi_N$ is symmetric (antisymmetric) under nuclear

interchange when the nuclear spin in integral (half-integral). Nuclear interchange is equivalent to changing the sign of $\vec{S}$, the internuclear vector. This implies that the symmetry of U_N is given by $(-1)^j$ where j is the rotational quantum number. Thus for the case of U_{el} symmetric, χ_N is symmetric (antisymmetric) for even (odd) j values, for the case of integral nuclear spin. For the case of half-integral nuclear spin, χ_N is antisymmetric (symmetric) for even (odd) j values.

If $\vec{I}$ is the nuclear spin quantum number for one of the identical nuclei, the total nuclear spin is given by $\vec{T}$:

$$T = 2I, 2I-1, \ldots, 0; \; m_T = T, \ldots, -T \qquad (2.8)$$

Of course, m_T is the projection of T on the z-axis. A state with a given T has a statistical weight of (2T+1). For even T and integral I, there are (2I+1)(I+1) values of (2T+1). For odd T and integral I, there are (2I+1)I values. The reverse is true for half-integral I. In both cases the (2I+1)(I+1) states are symmetric and the (2I+1)I states are antisymmetric. Thus the ratio of symmetric spin states to antisymmetric spin states is (I+1)/I. As a result, for a gas of homonuclear diatomics in statistical equilibrium, the ratio of the number of

molecules with even j to the number with odd j is (I+1)/I if I is integral and I/(I+1) is I is half-integral.

For H_2, I=1/2 and the possible T values are 1, 0. T=1 describes antisymmetric spin levels and T=0 describes symmetric spin levels. The ratio of symmetric spin states to antisymmetric spin states is, since U_{el} is symmetric with respect to interchange of nuclei, 1:3. The T=1 state of H_2 is called orthohydrogen and T=0 is called parahydrogen. Thus the even j rotational levels are characteristic of para and odd j rotational levels of ortho. As a result, the odd j levels occur three times more frequently than the even j values.

C. Rotational and Vibrational States

The nuclear Hamiltonian in Eq. (2.5) is the sum of a rotational part and a vibrational part. In the first approximation we assume that the motions are not coupled. Thus the rotational part of the Hamiltonian describes a rigid rotator. The SE for a rigid rotator is

$$\left[\frac{1}{\sin\theta} \frac{\partial}{\partial\theta} \sin\theta \frac{\partial}{\partial\theta} + \frac{1}{\sin^2\theta} \frac{\partial^2}{\partial\phi^2} + 2IE_j \right] Y_j^{\pm m_j}(s) = 0 \qquad (2.9)$$

where the solutions are spherical harmonics with energy eigenvalues given by $E_j = \frac{1}{2I} j(j+1)$, in units of $\hbar$.

The vibrational part of the Hamiltonian in (2.5) reduces to

$$(\frac{d^2}{ds^2} + 2u[E_v - U(s)])Z_v(s) = 0 \qquad (2.10)$$

and is thus a harmonic oscillator equation except for the fact that $Z_v(s)$ depends parametrically on the electronic energy $U(s)$. The energy eigenvalues are given by $E_v = \nu_o(v+\frac{1}{2})$, where ν_o is a constant.

D. Electronic States

In molecules, there is no conservation of total orbital angular momentum because the electric field of more than one nucleus is not spherically symmetric. In diatomic molecules there does exist an axial symmetry about the line joining the two nuclei. This implies that the projection of the total angular momentum of the electrons, on this axis is conserved. It is usually labeled by $\Omega=0,1,2,\ldots$. The symbols used to represent these values of Ω are respectively Σ, π, Δ.

The total spin, S, of all the electrons is conserved and (2S+1) gives the term multiplicity as it does for atoms; e.g. $^1\Sigma$ is a singlet term with $\Omega=0$.

The energy of the molecule is unchanged upon reflection of electronic coordinates in a plane containing the internuclear axis. However, the sign of the electronic

angular momentum does change. Thus states with non-zero Ω values are doubly degenerate; hence the terminology Ω-doubling. For Σ terms, the state is not changed. The wave function can only be multiplied by a constant upon reflection. Since a double reflection is the identity operator, the constant must be ± 1. Thus the Σ wave-function either changes sign, Σ^-, or doesn't change sign Σ^+.

For homonuclear diatomics, as has been indicated already, there is an additional symmetry plane, perpendicular to the internuclear axis, and passing through the center of the axis. The energy is invariant with respect to reflections in this plane and thus the wave function changes sign, Σ_u, or doesn't change sign Σ_g upon reflection of the state in the symmetry plane.

There is a useful empirical rule that the ground electronic state of a diatomic molecule is described by $^1\Sigma^+$, and if in addition it is homonuclear, $^1\Sigma_g^+$, as is the case for H_2. An important exception is O_2 which has a ground state $^3\Sigma_g^-$.

E. The Molecular Symmetric Top[4]

In writing the rotational and vibrational wave functions, it was assumed that the rotational motion was uncoupled from the electronic motion. In order to get a better feeling for the meaning of this assumption, we for

the moment, relax it and look at the molecule as a symmetric top. Thus we regard the diatomic as a rigid rotator with a rigid electron cloud "flywheel"[4] mounted on each end. The classical dynamics of this system, is that of a symmetric top. The moment of inertia about the internuclear axis, caused by the electron cloud, is much smaller than the moment of inertia about an axis perpendicular to the internuclear axis; however, because of the greater velocity of the electrons, the angular momentum from each of the two moments are of the same order. One then wonders how it is possible to assume the motions are uncoupled. We shall attempt to explain.

Let us call the vector sum of the electronic angular momentum and the nuclear angular momentum, $\vec{P}$. $\vec{P}$ is a constant of the internal motion. Its projection onto the internuclear axis, Ω, is quantized and is constant in magnitude but not in direction. Let us define $\vec{J}=\vec{P}+\vec{S}$; $|\vec{J}|=J(J+1)$ in units of $\hbar$. Figure 2a is a diagram of the angular momentum vectors of a symmetric top, after Herzberg.[4] The component of $\vec{J}$ perpendicular to the internuclear axis is given by $\vec{N}$. Thus since $\vec{J}$, $\vec{\Omega}$ are quantized, $\vec{N}$ is not. We see that $\vec{J}\cdot\vec{S}=0$ only when $\Omega=0$ implying that $\vec{J}=\vec{N}$. So physically then, when $\Omega=0$, the effects of electron angular momentum cancel and $\vec{J}$ has the same direction as for a rigid rotator. Thus for the purpose of calculating

rotational wave functions, the motion is effectively uncoupled for $\Omega=0$.

The uncoupling of the vibrational and electronic motion is a much more accurate assumption for low vibrational states, than rotational-electronic uncoupling. However, as we have indicated during collision processes, these assumptions are not apriori still operative. Realizing this, for later reference, we consider for non-$\Omega=0$ states, two different types of rotational-electronic coupling, for bound-state molecular systems, called Hund's cases "b" and "d".

Disregarding nuclear spin, since its only effect is to decouple H_2 into ortho and para modifications, essentially noninteracting, $\vec{J}$ is the total angular momentum of the molecule. For light molecules, the spin vector, $\vec{S}$, is only weakly coupled to the internuclear axis; this weak coupling characterizes Hund's case b as in Figure 2b. In this case, the projection of the electronic angular momentum on the internuclear axis, $\vec{\Omega}$, and the component of $\vec{J}$ perpendicular to the internuclear axis, $\vec{N}$, are added

$$\vec{K} = \vec{\Omega} + \vec{N}$$

$$|\vec{K}| = \Omega, \Omega+1, \ldots \qquad (2.11)$$

$\vec{K}$ is assumed in this case to be the total angular momentum. If $\Omega=0$, $\vec{K}$ is the same vector as $\vec{N}$, and in this case

$$\Omega = 0 \neq \vec{K} = \vec{N} \equiv j$$

[the rotational quantum number is j]

(2.12)

In the situation where the electronic orbital angular momentum is weakly coupled to the internuclear axis, and is strongly coupled to the rotation axis, we define Hund's case d. The angular momentum of nuclear rotation, we now call $\vec{R}$ instead of $\vec{N}$, because $\vec{R}$ is quantized with values $\sqrt{R(R+1)}$. When $\Omega=0$, $\vec{R}=\vec{j}$. In this case the total angular momentum (apart from spin) is

$$\vec{K} = \vec{R} + \vec{L}$$

$$K = |\vec{R}-\vec{L}|, \ |\vec{R}-\vec{L}|+1, \ \ldots, \ \vec{R}+\vec{L}$$

$\vec{L}$ = electronic angular momentum (2.13)

We shall find that the frame transformation in e^{-}-H_2 scattering corresponds to transitions of the type involved in transitions from Hund's case b (body) to Hund's case d (lab).

CHAPTER III

DYNAMIC AND FIXED NUCLEI APPROXIMATIONS

A. Lab Frame Close-Coupling Equations

The laboratory frame treatment of e^--H_2 scattering might well be called the dynamic nuclei approximation. Basically, the approximation assumes that the period of nuclear motion is much less than the electron-molecule interaction time. This is a reasonable assumption for a 0-10 eV projectile; however, we see possible problems resulting from projectile accelerations.

The SE of the H_2 molecule is given by[10]

$$[\hat{H}(\vec{r}_1,\vec{r}_2;\vec{S})-E_\alpha]\psi_\alpha(\vec{r}_1,\vec{r}_2;\vec{S}) = 0 \qquad (3.1)$$

where

$$\alpha = \{n,\Omega,S,M_S,v,j,m_j\} \qquad (3.2)$$

where n defines the symmetry character, Ω is the projection of the electronic angular momentum on the internuclear axis $\vec{S}$, S is the spin and M_S the magnetic spin quantum number. The positions of the two molecular electrons are given by $\vec{r}_1$, $\vec{r}_2$; the vibrational and rotational quantum numbers are v, j; and E_α is the total discrete energy of

the molecule in state Ψ_α. Considering only Σ states so that there is no Ω-doubling and using the Born-Oppenheimer Approximation

$$\Psi_\alpha(\vec{r}_1,\vec{r}_2;\vec{S}) = \psi_{n\Omega}(\vec{r}_1,\vec{r}_2,\vec{S})\chi_{SM_S}(1,2)Z_{n\Omega Sv}(S)R_{j\Omega m_y}(\hat{S}) \tag{3.3}$$

where (ψ) is the spatial part, (χ) is the spin part, (Z) is the vibration part, and (R) is the rotation part.

Then the SE representing the scattering process is

$$[H_T - E_T]\Psi_T = 0$$

$$H_T = T_3 + V_3(\vec{r}_1,\vec{r}_2,\vec{r}_3;\vec{S}) + H(\vec{r}_1,\vec{r}_2;\vec{S}) \tag{3.4}$$

In (3.4) "three" labels the projectile electron and T_3 represents the kinetic energy operator; V_3 represents the interaction between the projectile and the molecule. The usual scattering boundary conditions apply. We assume that the wave function Ψ_T is completely antisymmetric in space and spin.

We now specialize to the lab frame and expand the total wave function as

$$\Psi_T = \Psi_u = \hat{A} \sum_{u'} \frac{1}{r_3} FL_{u'u}(r_3)\Psi_{\alpha'}(\vec{r}_1,\vec{r}_2;\vec{S})Y_{\ell'm_{\ell'}}(\hat{r}_3)\chi_{m_{s'}}(3)$$

$$u = [\alpha,\ell,m_\ell,m_s] \tag{3.5}$$

where $\hat{A}$ is the antisymmetrization operator, ℓ and m_ℓ are angular momentum quantum number and corresponding magnetic quantum number of the projectile electron. The spin quantum number of the projectile is s and its projection is m_s and thus $\chi_{m_s'}^{(3)}$ is the spin function of the projectile. $FL_u(r_3)$ is the radial function describing the projectile and $Y_{\ell m_\ell}(r_3)$ is the spherical harmonic describing the angular behavior of the projectile. Following Arthurs and Dalgarno,[7] $\vec{\ell}$ and $\vec{j}$ are coupled to give a total angular momentum $\vec{J}$ which commutes with H_T. This is quite analogous to Hund's case (d); see Fig. 2c. Similarly, $S_T=\vec{S}+\vec{s}$. We thus form two new functions[6]

$$\Phi_\gamma = \Phi_{j\Omega\ell}^{JM}(\hat{r}_3,\hat{S}) = \sum_{m_j,m_\ell} C(j\ell J;m_j m_\ell m_J)Y_{\ell m_\ell}(\hat{r}_3)$$

$$* R_{j\Omega m_j}(\hat{S}) \tag{3.6}$$

where

$$\gamma = [n,\Omega,S,v,j,\ell,J,m_J,S_T,m_{S_T}] \tag{3.7}$$

and the C-function is a Clebsch-Gordon coefficient and

$$\chi_\gamma = \chi^{S_T m_{S_T}}_{S\,1/2}(1,2,3) = \sum_{m_S, m_s} C(SsS_T; m_S m_s m_{S_T})$$

$$\chi_{Sm_S}(1,2)\chi_{m_s}(3) \qquad (3.8)$$

Thus during the collision, J, m_j, S_T, m_{S_T} are conserved and the radial functions are independent of m_j, m_{S_T}. Including the new functions

$$\Psi_T = \Psi_\gamma = \hat{A} \sum_{\gamma'} \frac{1}{r_3} FL_{\gamma',\gamma}(r_3)\psi_{n\Omega}(\vec{r}_1,\vec{r}_2,S)Z_v(S)$$

$$\Phi_\gamma(\hat{r}_3,\hat{S})\chi^{S_T m_{S_T}}_{S\,1/2}(1,2,3) \qquad (3.9)$$

where we have assumed Z independent of n,Ω,S. Taking (3.9) and plugging it into (3.4), we multiply by

$$[\psi_{n\Omega}\ \chi^{S_T m_{S_T}\ \dagger}_{S\,1/2}(1,23)]$$

and integrate over $d\vec{r}_1 d\vec{r}_2$ and sum over spin, where

$$\chi^{S_T m_{S_T}}_{S\,1/2}(1,2,3) = \frac{1}{\sqrt{2}}[\alpha(1)\beta(2)-\alpha(2)\beta(1)]\alpha(3) \qquad (3.10)$$

is the doublet spin function. Finally, assuming

$$\int d\vec{r}\; r\; \psi_{n\Omega}(\vec{r}_1,\vec{r},\vec{S}) FL_{\gamma\gamma'}(r) = 0 \qquad (3.11)$$

we obtain[6]

$$\left[\frac{d^2}{dr_3^2} - \frac{\ell_i(\ell_i+1)}{r_3^2} + k_i^2\right] FL^{\ell_i j_i v_i}_{\ell_k j_k v_k}(r_3)$$

$$- 2 \sum_{\ell_j j_j v_j} \left\{ \int d\hat{r}_3\, d\vec{S}\; \Phi^*_{\ell_i j_i}(\hat{r}_3,\hat{S}) Z_{v_i}(S) \bar{V}_d(\vec{r}_3,\vec{S}) \right.$$

$$\left. Z_{v_j}(S) \Phi_{\ell_j j_j}(\hat{r}_3,\hat{S}) \right\} FL^{\ell_j j_j v_j}_{\ell_k j_k v_k}(r_3)$$

$$+ 2 \sum_{\ell_j j_j v_j} \int_0^\infty dr_1\; FL^{\ell_j j_j v_j}_{\ell_k j_k v_k}(r_1)$$

$$K(\ell_i j_i v_i, \ell_j j_j v_j; J | r_1, r_3) = 0 \qquad (3.12a)$$

where we have dropped extraneous indices and

$$k_i^2 = B j_i(j_i+1) + \nu_o(v_i+\tfrac{1}{2}) - E$$

$$B = \text{rotational constant}$$

$$\nu_o = \text{vibrational constant}$$

$$E = \text{projectile kinetic energy} \qquad (3.12b)$$

The direct potential is

$$\bar{V}_d(\vec{r}_3,\vec{S}) = \int d\vec{r}_1 d\vec{r}_2 \psi_o^*(\vec{r}_1,\vec{r}_2,\vec{S}) V_3(\vec{r}_1,\vec{r}_2,\vec{r}_3;\vec{S}) \psi_o(\vec{r}_1,\vec{r}_2,\vec{S}) \tag{3.13}$$

and the exchange kernel is

$$K(\ell_i j_i v_i, \ell_j j_j v_j; J|r_1,r_3) = r_1 r_3 \int d\hat{r}_1 d\hat{r}_2 d\hat{r}_3 d\vec{s}$$

$$(\Phi^*_{\ell_i j_i}(\hat{r}_3,\hat{S}) Z_{v_i}(S) \psi_o^*(\vec{r}_1,\vec{r}_2,\vec{S}) \frac{1}{r_{13}} \psi_o(\vec{r}_2,\vec{r}_3,\vec{S})$$

$$\Phi_{\ell_j j_j}(\hat{r}_1,\hat{S}) Z_{v_j}(S) \tag{3.14}$$

where we have assumed the molecule is in its ground electronic state $\psi_{n\Omega}=\psi_o$.

The boundary conditions for (3.12) are

$$FL^{\ell_i j_i v_i}_{\ell_k j_k v_k}(0) = 0$$

$$FL^{\ell_i j_i v_i}_{\ell_k j_k v_k}(r) \begin{cases} \underset{r\to\infty}{\sim} \sin(k_i r - \frac{1}{2}\ell_i\pi)\delta_{ik} \\ \quad + \cos(k_i r - \frac{1}{2}\ell_i\pi) R_{ik} \quad ; \quad k_i^2 > 0 \\ \underset{r\to\infty}{\sim} \exp(-|k_i| r) \quad ; \quad k_i^2 < 0 \end{cases} \tag{3.15}$$

The total cross-sections are given by

$$\sigma(v_k j_k \to v_i j_i) = \frac{\pi}{(2j_k+1)k_i^2} \sum_{J=0} \sum_{\ell_i,\ell_k} (2J+1)$$

$$|T^J(\ell_k j_k v_k, \ell_i j_i v_i)|^2 \qquad (3.16)$$

where the T-matrix is related to the R-matrix via

$$\underline{T} = 2i\ \underline{R}/(\underline{1}-i\underline{R}) \qquad (3.17)$$

The differential cross sections, averaged over m_{j_k} and summed over m_{j_i} are given by[7]

$$\frac{d\sigma}{d\theta}(v_k j_k \to v_i j_i|\theta) = \frac{\pi(-1)^{j_i-j_k}}{2(2j_k+1)k_i^2} \sum_{\lambda=0}^{\infty} A_\lambda P_\lambda(\cos\theta) \qquad (3.18)$$

where

$$A_\lambda = \sum_{J_1=0}^{\infty} \sum_{J_2=0}^{\infty} \sum_{\ell_1=|J_1-j_k|}^{J_1+j_k} \sum_{\ell_2=|J_2-j_k|}^{J_2+j_k} \sum_{\ell_1'=|J_1-j_i|}^{J_1+j_i} \sum_{\ell_2'=|J_2-j_i|}^{J_2+j_i}$$

$$* \; Z[\ell_1' J_1 \ell_2' J_2; j_i \lambda] \; Z[\ell_1 J_1 \ell_2 J_2; j_k \lambda]$$

$$* \; T^{J_1}(j_i \ell_1'; j_k \ell_1) \; T^{J_2}(j_i \ell_2'; j_k \ell_2) \qquad (3.19$$

and

$$Z(abcd;ef) = (-1)^{1/2(f-a+c)} [(2a+1)(2b+1)(2c+1)(2d+1)]^{1/2}$$

$$* \; C(aco;foo) \; W[abcd;ef] \qquad (3.20)$$

where W is a Racah coefficient.

B. Lab Frame Potentials

In the evaluation of the exchange potential, we follow Ardill and Davison[8] as Henry and Lane did[17]; the equations (3.12) then become

$$\left[\frac{d^2}{dr^2} - \frac{\ell_i(\ell_i+1)}{r^2} + k_i^2 \right] FL_{ik}(r)$$

$$- 2 \sum_{\ell_j j_j v_j} \left\{ \int d\hat{r} d\hat{S} \; \Phi^*_{\ell_i j_i}(\hat{r},\hat{S}) Z_{v_i}(S) \bar{V}_d(\vec{r},\vec{S}) Z_{v_j}(S) \right.$$

$$\left. \Phi_{\ell_j j_j}(\hat{r},\hat{S}) \right\} FL_{jk}(r)$$

$$+ 2 \sum_{\alpha_i} EL(\ell_i j_i, \alpha_i) \; P_{t'}(r) Y_\lambda [P_t(y) \; FL_{nk}(y); r] = 0$$

(3.21)

where

$$k_i^2 = E + Bj_i(j_i+1)$$

$$B = 1/2I \; ; \quad I = \text{moment of inertia}$$

$$\alpha_i = \{\ell n, j_n, \lambda, t, t'\}$$

$$P_t(r) = \text{one particular term of the electronic bound-state wave function} \qquad (3.22)$$

Following Henry and Lane we use the Huzinaga wave function[18] for the $^1\Sigma_g^+$ state of H_2 and obtain

$$t = \{1s, 2s\}$$

$$P_{1s} = 1.13050r \exp(-1.1r) + 20.51813r^4 \exp(-4.3r)$$

$$P_{2s} = 1.43108r \exp(-0.8r)$$

$$EL(\ell_i j_i, 1s, 1s) = ba_{1s}/(2\ell_i+1)$$

$$EL(\ell_i j_i, 1s, 2s) = b/(2\ell_i+1)$$

$$EL(\ell_i j_i, 2s, 1s) = b/(2\ell_i+1)$$

$$EL(\ell_i j_i, 2s, 1s) = ba_{2s}/(2\ell_i+1)$$

$$b = 0.33305$$

$$a_{1s} = 0.49561/0.33305$$

$$a_{2s} = 0.27181/0.33305 \qquad (3.23)$$

and

$$V_\lambda[P_t(y)FL_{nk}(y);r] = \frac{1}{r^{\lambda+1}}\int_o^r dy\ y^\lambda\ P_t(y)FL_{nk}(y)$$

$$+ r^\lambda \int_r^\infty dy\ \frac{1}{y^{\lambda+1}}\ P_t(y)FL_{nk}(y) \qquad (3.24)$$

Note the Huzinaga wave functions are independent of S and thus using

$$\int ds\ Z_{v_i}(s)Z_{v_j}(s) = \delta_{v_i v_j} \qquad (3.25)$$

the exchange term is independent of S.

Following Henry[6] we expand

$$\bar{V}_d(\vec{r},\vec{s}) = \sum_\lambda v_\lambda(r,s)P_\lambda(\hat{r}\cdot\hat{s}) \qquad (3.26)$$

Thus the direct potential matrix element becomes

$$\sum_\lambda fL_\lambda(j_i\ell_i,j_j\ell_j;J)\int_o^\infty ds\ Z_{v_i}(s)v_\lambda(r,s)Z_{v_j}(s)$$

(3.27)

where

$$fL_\lambda(j_i\ell_i,j_j\ell_j;J) = \frac{(-1)^{j_i+j_j-J}}{(2\lambda+1)}\,[(2j_i+1)(2\ell_i+1)$$

$$(2j_j+1)(2\ell_j+1)]^{1/2}$$

$$* \; W[j_i\ell_i,j_j\ell_j;J\lambda]\; C(\ell_i\ell_j\lambda;ooo)\; C(j_ij_j\lambda;ooo) \qquad (3.28)$$

The short-range part of v is given by

$$v_\lambda(r,s) = (2\lambda+1)\int_{-1}^{+1} dt\,\left[\frac{1}{[r^2+\frac{1}{4}s^2+rst]^{1/2}} + Z(s)\right]$$

$$* \exp\{-2Z(s)[r^2+s^2/4 + rst]^{1/2}\}\; P_\lambda(t) \qquad (3.29)$$

where

$$Z(s) = 1 + (0.863-0.319s)\exp(-0.641s) \qquad (3.30)$$

The long range part includes the quadrapole term

$$v_2^Q(r,s) = -Q(s)\,\frac{1}{r^3}\,[1-\exp(-(r/r_o)^6)] \qquad (3.31)$$

and the polarization terms

$$v_o^P(r,s) = -[\alpha_o(s)/2(r^2+r_1^2)^2]\{1-\exp[-(r/r_a)^3]\} \qquad (3.32)$$

$$v_2^P(r,s) = -[\alpha_2(s)/2(r^2-r_2^2)]\{1-\exp[-(r/r_b)^4]\}$$

(3.33)

where r_1, r_2, r_a, r_b are given by 1.22, 0.1, 1.7, 2.0 a_o. The functions $Q(s)$, $\alpha_o(s)$, $\alpha_2(s)$ averaged over initial and final vibrational states are given in Table 1.

C. Body Frame Close-Coupling Equations

The basic idea of the body frame approach is that the projectile electron completely traverses the interaction region before the target molecule has a chance to react to the force due to its presence. This in itself gives a qualitative idea of the limitations inherent in its application. The difference from the lab frame approach springs from the angular functions used to describe the projectile; see Fig. 3. The body frame expansion of the total wave function, correspondent to Eq. (3.9) is

$$\Psi_T = \hat{A} \sum_{\ell'\Omega'} \frac{1}{r_3} FB^{J\eta}_{\substack{\ell'\Omega' \\ \ell\Omega}}(r_3,s)\psi_o(\vec{r}_1,\vec{r}_2,s)\chi^{Jm\eta}_{\ell'\Omega'}(\hat{r}_3,\hat{s});$$

$$\eta = (\pm) \qquad (3.34)$$

The angular functions (χ) are eigenfunctions of the operator projecting the projectile's angular momentum on

the internuclear axis, $\hat{\Omega}^2 = (\vec{\ell}\cdot\hat{s})^2$. The $(\pm)$ represents the symmetry of the molecular electronic wave function upon reflection in a plane containing the molecular axis; thus it is a characteristic of the Σ states. For the $^1\Sigma_g^+$ electronic H_2 ground state, the only term that occurs is the (+) term. The χ-functions are obtained by rotating the spherical harmonic lab angular functions to the body frame. They are given by[20]

$$\chi^{JM}_{\ell\Omega}(\hat{r},\hat{s}) = \left[\frac{2J+1}{8\pi(1+\delta_{\Omega o})}\right]^{1/2} \left[Y^{\Omega}_{\ell}(\theta_r,\phi_r)D^{d}_{\Omega m}(0,\theta_s,\phi_s)\right.$$

$$\left. + \eta\, Y^{-\Omega}_{\ell}(\theta_r,\phi_r)D^{J}_{-\Omega m}(0,\theta_s,\phi_s)\right] \qquad (3.35)$$

where

(θ_r,ϕ_r) = electron coordinates

(θ_s,ϕ_s) = internuclear axis coordinates

and

$$D^{J}_{\Omega m}(0,\theta_s,\phi_s) = e^{-im\phi_s} \sum_K (-1)^K \frac{[(J+M)!(J-M)!(J+\Omega)!(J-\Omega)!]^{1/2}}{K!(J+M-K)!(J-\Omega-K)!(K+\Omega-M)!}$$

$$* \left[\cos\frac{\theta_s}{2}\right]^{2J-2K-\Omega+M} \left[-\sin\frac{\theta_s}{2}\right]^{2K+\Omega-M} \qquad (3.36)$$

We note that

$$\int d\hat{r}d\hat{s}\; X^{JM\eta *}_{\ell_i\Omega_i}(\hat{r},\hat{s})\; X^{JM}_{j\ j}(\hat{r},\hat{s}) = \delta_{\ell_i\ell_j}\,\delta_{\Omega_i\Omega_j} \tag{3.37}$$

Plugging (3.34) into (3.4), we obtain[12]

$$\left[\frac{d^2}{dr_3^2} - \frac{\ell_i(\ell_i+1)}{r_3^2} - E\right] FB^{\ell_i\Omega_i}_{\ell_k\Omega_k}(r_3,s)$$

$$-2\sum_{\ell j}\left\{\int d\hat{r}d\hat{s}\; X^{*}_{\ell_i\Omega_i}(\hat{r},\hat{s})\bar{V}_d(\vec{r},\vec{s})X_{\ell_j\Omega_i}(\hat{r},\hat{s})\right\}FB^{\ell_j\Omega_i}_{\ell_k\Omega_k}(r_3,s)$$

$$-2\sum_{\Omega j}\left\{d\hat{r}d\hat{s}\; X^{*}_{\ell_i\Omega_i}(\hat{r},\hat{s})\hat{H}_{rot.}(s)X_{\ell_i\Omega_j}(\hat{r},\hat{s})\right\}FB^{\ell_i\Omega_j}_{\ell_k\Omega_k}(r_3,s)$$

$$-2\sum_{vj}\hat{H}_{vib}(s)Z_{v_j}(s)\int ds'\; Z_{v_j}(s')FB^{\ell_i\Omega_i}_{\ell_k\Omega_k}(r_3,s')$$

$$+2\sum_{\ell_j\Omega_j}\int d\vec{r}_1\; K(\ell_i\Omega_i,\ell_j\Omega_j;JM|\,r_1,r_3;s)FB^{\ell_j\Omega_j}_{\ell_k\Omega_k}(r,s) = 0 \tag{3.38a}$$

where

$$K(\ell_i\Omega_i,\ell_j\Omega_j;JM|\,r_1,r_3;s) =$$

$$\int d\hat{r}_3\int d\vec{r}_2\; X^{*}_{\ell_i\Omega_i}(\hat{r}_3,\hat{s})\psi_o(\vec{r}_1,\vec{r}_2,s)\;\frac{1}{r_{32}}\;\psi_o(\vec{r}_3,\vec{r}_2,s)$$

$$*\,X_{\ell_j\Omega_j}(\hat{r}_3,\hat{s}) \tag{3.38b}$$

where we have eliminated unnecessary symbols such as η since we are assuming for this problem $\eta=+1$.

D. Body-Frame Potentials

The direct potential is expanded as it was in the lab frame, Eq. (3.26),

$$\bar{V}_d(\vec{r},\vec{s}) = \sum_\lambda v_\lambda(r,s) P_\lambda(\hat{r}\cdot\hat{s}) \tag{3.39}$$

Then the potential matrix becomes

$$\sum_\lambda fB_\lambda(\Omega_i \ell_i, \Omega_i \ell_j) v_\lambda(r,s) \tag{3.40}$$

Note (3.40) is diagonal in Ω, η, J, m. Then

$$fB_\lambda(\Omega_i \ell_i, \Omega_j \ell_j) = \left[\frac{(2\ell_j+1)}{(2\ell_i+1)}\right]^{1/2} C(\ell_j \Omega_i \ell_i; \Omega_j O \Omega_i) * C(\ell_j \Omega_i \ell_i; 000) \tag{3.41}$$

It can be shown using the frame transformation introduced in the next chapter that, using the Wang wave function[19] as we did for the lab, the exchange term is exactly of the same form. In practice the rotational and vibrational terms are dropped. We'll talk more about this in the next chapter. However, the rotational term is used in determining the conditions for the rotational

transformation and will be evaluated in the next chapter. The body frame equations that are integrated are given by

$$\left[\frac{d^2}{dr^2} - \frac{\ell_i(\ell_i+1)}{r^2} + E\right] FB^{\ell_i\Omega_i}_{\ell_k\Omega_k}(r)$$

$$- 2 \sum_{\ell_j} \sum_{\lambda} fB_\lambda(\Omega_i\ell_i,\Omega_i\ell_j) FB^{\ell_j\Omega_i}_{\ell_k\Omega_k}(r)$$

$$+ 2 \sum_{\alpha} EB(\ell_i\Omega_i,\alpha) P_\beta(r) Y_{\ell_i}\left[P_\tau(y) FB^{\ell_i\Omega_i}_{\ell_k\Omega_k}(y);r\right] = 0 \qquad (3.42)$$

where $\alpha = \{\beta,\tau\}$ and $\beta,\tau = \{1,2\}$ and Y_{ℓ_i}'s are defined as in the lab frame. Also the functional form of EB is the same as EL given by (3.23).

CHAPTER IV

THE FRAME TRANSFORMATION

The transformation between the eigenstates of j^2 and $\Omega^2=(\vec{\ell}\cdot\vec{s})^2$ is a unitary matrix with elements labeled by[20] $U_{j\Omega}^{(\ell J\eta)}$. Thus

$$\chi_{\ell\Omega}^{Jm\eta}(\hat{r}',\hat{s}') = \sum_j U_j^{(\ell J\eta)} \Phi_{\ell j}^{Jm\eta}(\hat{r},\hat{s}) \qquad (4.1)$$

We proceed to define the matrix elements themselves and the limits of the sum over j.

The lab angular functions are (see 3.6)

$$\Phi_{\ell j}^{Jm\eta}(\hat{r},\hat{s}) = \sum_m C(\ell jJ;m,M-m,M) Y_{\ell m}(\hat{r}) Y_{jM-m}(\hat{s}) \qquad (4.2)$$

where the R↛Y because the molecule is a simple rotor. The body frame angular functions are (see 3.35)

$$\chi_{\ell\Omega}^{JM\eta}(\hat{r}',\hat{s}') = \left[\frac{2J+1}{8\pi(1+\delta_{\Omega O})}\right]^{1/2} \left[Y_{\ell\Omega}(\hat{r}') D_{\Omega M}^{J}(0,\hat{s}')\right.$$

$$\left. + \eta\, Y_{\ell,-\Omega}(\hat{r}') D_{-\Omega M}^{J}(0,\hat{s}')\right] \qquad (4.3)$$

where the prime refers to the body frame coordinates. The D^J functions are wave functions of the symmetric rotor.[21] The transformation of the spherical harmonics is

$$Y_{\ell\Omega}(\hat{r}') = \sum_m Y_{\ell m}(\hat{r}) D^{\ell}_{m\Omega}(-\pi-\phi,\theta,\pi) \qquad (4.4)$$

Let us note that the D^J's are defined with Euler angles in the negative sense according to the right-hand rule. Also, if the set of Euler angles is α, β, γ, we see from (4.3) that $\alpha=0$ because we are only interested in aligning, through a set of rotations, the Z'-axis with the internuclear axis, and we are not interested in the direction of the x', y' axes because of the axial symmetry of H_2. We then substitute (4.4) into (4.3) and (4.3) into (4.1) to obtain

$$\left[\frac{2J+1}{8\pi(1+\delta_{\Omega O})}\right]^{1/2} \{ [\sum_m Y_{\ell m}(\hat{r}) D^{\ell}_{m\Omega}(-\pi-\phi,\theta,\pi)] D^J_{\Omega m}(O,\hat{s})$$

$$+ \eta [\sum_m Y_{\ell m}(\hat{r}) D^{\ell}_{m,-\Omega}(-\pi-\phi,\theta,\pi)] D^J_{-\Omega m}(O,\hat{s}) =$$

$$\sum_j U^{(\ell J\eta)}_{j\Omega} \Phi^{Jm\eta}_{\ell j}(\hat{r},\hat{s}) \qquad (4.5)$$

Note two facts about the D^J's;

$$D^{\ell}_{m\Omega}(-\pi-\phi,\theta,\pi) = (-1)^{\Omega-m} D^{\ell}_{-\Omega-m}(O,\hat{s}); \quad \hat{s} = (\theta,\phi)$$

$$(4.6)$$

$$D^j_{O,M-m}(O,\hat{s}) = Y_{jM-m}(\hat{s}) \left[\frac{4\pi}{2j+1}\right]^{1/2} \qquad (4.7)$$

Using

$$\int \hat{dr}\hat{ds}\ \Phi^{*JM\eta}_{\ell' j'}(\hat{r},\hat{s})\ \Phi^{JM\eta}_{\ell j}(\hat{r},\hat{s}) = \delta_{\ell\ell'}\ \delta_{jj'} \qquad (4.8)$$

along with

$$D^{\ell}_{m\Omega}(-\pi-\phi,\theta,\pi)\ D^{J}_{\Omega M}(0,\theta,\phi) = \sum_{j} C(\ell Jj;\ell-\Omega,\Omega,0)$$

$$\cdot\ D^{j}_{0,M-m}(0,\theta,\phi)\ C(\ell Jj;\ell-m,M,M-m) \qquad (4.9)$$

one obtains

$$U^{\ell J\eta}_{j\Omega} = \left[\frac{2j+1}{2J+1}\right]^{1/2} C(\ell jJ;\Omega 0\Omega)\ \frac{1+\eta(-1)^{J-j-\ell}}{[2(1+\delta_{\Omega 0})]^{1/2}}$$

$$= (-1)^{J+\Omega-j}\ C(\ell Jj;\ell-\Omega,\Omega,0)\ \frac{1+\eta(-1)^{J-j-\ell}}{[2(1+\delta_{\Omega 0})]^{1/2}} \qquad (4.10)$$

The dimensions of the U matrix are defined by the following

$$L = \min(\ell,J)$$

$$\eta = (+) \ddagger \quad j = |J-\ell|, |J-\ell|+2, \ldots, J+\ell$$

$$\Omega = 0,1,\ldots,L$$

$$\eta = (-) \neq j = |J-\ell|+1, |J-\ell|+3, \ldots, J+\ell-1$$
$$\Omega = 1, \ldots, L \tag{4.11}$$

In general, the number of body frame channels (NB) is less than the number of lab frame channels (NL). In matrix notation the lab frame equations can be written

$$\begin{bmatrix} {}^{L}L_{11} & {}^{L}L_{12} & \cdots\cdots \\ {}^{L}L_{21} & {}^{L}L_{22} & \cdots\cdots \\ \cdot & \cdot & \cdot \\ \cdot & \cdot & \cdot \\ \cdot & \cdot & {}^{L}L_{NL,NL} \end{bmatrix} \begin{bmatrix} {}^{F}L_{11} & {}^{F}L_{12} & \cdots\cdots \\ {}^{F}L_{21} & {}^{F}L_{22} & \cdots\cdots \\ \cdot & \cdot & \cdot \\ \cdot & \cdot & \cdot \\ \cdot & \cdot & {}^{F}L_{NL,NL} \end{bmatrix} = 0 \tag{4.12}$$

Thus (4.12) may symbolically be written

$$[\underline{LL}][\underline{FL}] = 0 \tag{4.13}$$

Similarly, the body frame equations may be written

$$[\underline{LB}][\underline{FB}] = 0 \tag{4.14}$$

The rotational transformation between the two frames is determined by the transformations between the two respective set of angular functions, (4.1). Also, the

rotational transformation does not change the number of channels. Thus multiplying (4.14) by the transformation matrix $\underline{U}$,

$$\underline{U}^{-1}\ \underline{LB}\ \underline{U}\ \underline{U}^{-1}\ \underline{FB} = 0 \tag{4.15}$$

where in accord with the required reversibility of real physically operations, $\underline{U}$ must be unitary

$$\underline{U}\ \underline{U}^{-1} = \underline{1} \tag{4.16}$$

In a similar fashion, the transformation from the s-dependent equations to the s-independent equations is represented by a $\underline{z}$-matrix, where its elements are defined by

$$FV(r)_{\ell_i \Omega_i v_i} = \int_o^\infty ds\ Z_{v_i}(s)\ FB_{\ell_i \Omega_i}(r,s) \tag{4.17}$$

where the "V" indicates that the rotation hasn't been performed yet. The reverse transformation is given by

$$FB_{\ell_i \Omega_i}(r,s) = \sum_{v_i} Z_{v_i}(s)\ FV_{\ell_i \Omega_i v_i}(r) \tag{4.18}$$

We define the full transformation matrix $\underline{T}$ by

$$\underline{T} = \underline{U}\ \underline{Z} \tag{4.19}$$

where

$$\underline{T} = \begin{bmatrix} Z_o \underline{U} & & 0 \\ & Z_1 \underline{U} & \\ 0 & & \ddots \end{bmatrix} \qquad (4.20)$$

Thus the transformation between the lab-frame and body-frame radial functions, with vibrations included, is defined by

$$FL_i = \sum_j T^{-1}_{ij} FB_j \qquad (4.21)$$

where the indices correspond to the set of quantum numbers required to define the functions in the various frames. You will notice that from Equation (4.17) to Equation (4.21), the solutions have been written with one set of indices. In the context of the NIIEM, the solutions are matrices. Also notice that the number of channels, after the vibrational transformation, is greater than the number of channels before, the number increasing by a multiplicative factor equal to the number of vibrational states, NVS, included in the close-coupling expansion. Therefore the dimensionf of the solution matrix become (NVS*NB) x (NVS*NB) where NB is the number of channels in the body frame, before the vibrational transformation.

As a result, the vibrational transformation for the case of matrix solutions is achieved by multiplying

Equation (4.15) on the left by $\underline{Z}^{-1}$, and on the right by Z;

$$\underline{Z}^{-1}\ \underline{U}^{-1}\ \underline{LB}\ \underline{U}\ \underline{Z}\ \underline{Z}^{-1}\ \underline{U}^{-1}\ \underline{FB}\ \underline{Z} = 0 \qquad (4.22)$$

Thus

$$\underline{LV} = \underline{U}^{-1}\ \underline{LB}\ \underline{U} \qquad (4.23)$$

$$\underline{FV} = \underline{U}^{-1}\ \underline{FB} \qquad (4.24)$$

and

$$\underline{LL} = \underline{Z}^{-1}\ \underline{LV}\ \underline{Z} \qquad (4.25)$$

$$\underline{FL} = \underline{Z}^{-1}\ \underline{FV}\ \underline{Z} \qquad (4.26)$$

In general, as discussed by Chang and Fano, the vibrational and rotational transformation can be done at different points in the integration mesh; see Figure 4. However, in this paper, the transformations are performed at the same point. This is because we wish to investigate what should be by far the most important affect: the various shifts of the vibrational transformation point. Essentially what we hope to do is include the effect of some of the higher projectile partial waves by transforming to the body frame when the projectile is near the molecule.

We thus believe that for small radial distances from the molecule, the body frame expansion converges faster than the lab frame expansion.

Examine Figure 4. This figure is similar to a figure given by Chang and Fano.[11] The difference is that they didn't assume that a potential would be used all the way into the origin. They envisioned a calculation beginning with a many-body calculation near the origin, out to some point r_o, where the many-body calculation yields starting values for the wave function for a potential calculation. They assume that electron exchange will not be included in the potential calculation. In this paper we use a potential all the way into the origin, including exchange.

Also, in this paper, r_1 and r_2 coincide. Thus we have broken the electron trajectory into two regions, A and B. One of the major problems is determination of a quantitative definition of the boundary. For the case of two regions, vibrational frame transformation criteria should be used to determine the boundary. Qualitatively, in region A, the rotational and vibrational potential terms are assumed to be small compared with the direct potential. In general, the transformation point will be different for each e^--H_2 partial wave and each projectile energy.

CHAPTER V

THE INTEGRAL EQUATION SOLUTION OF THE CLOSE-COUPLING EQUATIONS

The close-coupling technique applied to a multi-channel scattering problem results in a set of coupled integro-differential equations for the continuum (scattering) functions

$$\left[\frac{d^2}{dr^2} - \frac{\ell_i(\ell_i+1)}{r^2} \pm (|k_i|)^2 + \frac{2(NZ-NE)}{r}\right] F_{ik}(r)$$

$$= \sum_{j=1}^{N} \left[V_{ij}(r) + \frac{2(NZ-NE)}{r}\right] F_{jk}(r) + \sum_{n=1}^{N} \left[\hat{W}_{in}(r) + \hat{Z}_{in}(r)\right] F_{nk}(r) + \sum_{\lambda=1}^{NORB} \delta_{\ell_i \ell_k} M_{\lambda}^{ik} P_{\lambda}(r) \; ; \; i,k = 1$$

where

N = number of channels

NE = number of negative charges in the target

NZ = number of positive charges in the target

ℓ_i = angular momentum in channel i

$\pm(|k_i|)^2$ = energy of the projectile in channel i referred to the lowest target state energy included in the close-coupling expansion in channel i for $\binom{\text{open}}{\text{closed}}$ channels.

NORB = number of orbitals describing the target

(5.1)

The $\underline{M}$ are undertermined Lagrange multipliers that insure that the solution $\underline{F}(r)$ is orthogonal to all the bound states, λ, of the target. Thus $P_\lambda(r)$ is the reduced radial part of the target orbital. The exchange potential is defined by

$$\sum_{n=1}^{N} \hat{W}_{in}(r)F_{nk}(r) = \sum_{\alpha_i}{}' B_i^{(\alpha_i)} Y_t[P_{\rho_i},F_{nk};r]\, P_{\rho_n}(r)$$

(5.2)

where

$$Y_t[A,B;r] = \frac{1}{r^{t+1}} \int_0^r dx\, A(x)B(x)X^t + r^t \int_r^\infty dx\, A(x)B(x)\, \frac{1}{x^{t+1}}$$

$$|\ell_{\rho_i} - \ell_n| \leq t \leq \ell_{\rho_i} + \ell_n$$

$$|\ell_{\rho_n} - \ell_i| \leq t \leq \ell_{\rho_n} + \ell_i$$

$$\alpha_i = \{t,i,n,\rho_i,\rho_n\} \qquad (5.3)$$

ℓ_{ρ_i} is the angular momentum of the target state ρ_i. The prime on the summation denotes a summation only over exchange terms. The $B_i^{(\alpha_i)}$ are the exchange potential coefficients. The correlation potential is given by

$$\sum_{n=1}^{N} \hat{Z}_{in}(r)F_{nk}(r) = \sum_{n}' \sum_{\zeta=1}^{NV} \left[\sum_{\nu=1}^{NV} E_{\zeta}^{\nu} V_{\nu i}(r) \right] \int_0^{\infty} dx\, V_{\zeta n}(x) F_{nk}(x) \tag{5.4}$$

where NV is the number of correlation terms in a channel, E_j^{ν} are the correlation constants, and $V_{\nu i}(r)$ are the correlation potential elements.

The Equation (5.1) are completely specified with the statement of the boundary conditions

$$F_{ik}(r) \begin{cases} \tilde{r \to 0} & 0 \\ \tilde{r \to \infty} & \dfrac{1}{[|k_i|]^{1/2}} \left[\delta_{ik} \sin\left(|k_i| r - \ell_i \dfrac{\pi}{2}\right) + R_{ik} \cos\left(|k_i| r - \ell_i \dfrac{\pi}{2}\right) \right] \end{cases} \tag{5.5}$$

As Smith and Henry[22] have shown, computation of the solutions of (5.1) may be facilitated by dropping certain normalization terms when the Eq. (5.1) is transformed to a Volterra integral equation of the second kind. The resulting solution satisfies

$$\psi_{ij}(r) \begin{cases} \underset{r\to 0}{\sim} 0 \\ \\ \underset{r\to\infty}{\sim} \dfrac{1}{[|k_i|]^{1/2}} [A_{ij} \sin(|k_i|r-\ell_i \frac{\pi}{2}) \\ \qquad + B_{ij} \cos(|k_i|r-\ell_i \frac{\pi}{2})] \end{cases} \qquad (5.6)$$

This solution (5.6) is called the unnormalized solution. The properly normalized solution (5.5) can be recovered from the unnormalized solution (5.6) at $r\sim\infty$ by multiplying from the right by $\underline{A}^{-1}$.

$$F_{ik}(r) = \sum_{j=1}^{N} \psi_{ij}(r) A_{jk}^{-1} \qquad (5.7)$$

Thus it is the unnormalized solution in the form of a Volterra integral equation of the second kind which is actually integrated.

$$\psi_{ik}(r) = \delta_{ik} G_i^{(1)}(|k_i|r) + \int_0^r dx\, G_i^{(2,1)}(r|x)$$

$$[\sum_n V_{in}(x)\psi_{nk}(x)$$

$$+ \sum'_{\alpha_i} B_i^{(\alpha_i)} P_{\rho_n}(x)\{\frac{1}{x^{t+1}} \int_0^x dy\, P_{\rho_i}(y)\psi_{nk}(y)$$

$$y^t - x^t \int_0^x dy\, P_{\rho_i}(y)\psi_{nk}(y)y^{-(t+1)}\}$$

$$+ \sum_n Z_{in}(x)\psi_{nk}(x) + \sum_\lambda \delta_{\ell_i \ell_\lambda} M_\lambda^{ik} P_\lambda(x)$$

$$+ \sum_{\alpha_i}{}' B_i^{(\alpha_i)} P_{\rho_n}(x) x^t \int_0^\infty dy\ P(y)\ \psi_{nk}(y) y^{-(t+1)}]$$

(5.8)

where

$$G_i^{(2,1)}(r|x) = G_i^{(2)}(|k_i|r) G_i^{(1)}(|k_i|x)$$

$$- G_i^{(1)}(|k_i|r) G_i^{(2)}(|k_i|x) \qquad (5.9)$$

with $G_i^{(1)}$, $G_i^{(2)}$ representing one dimensional coordinate-space Green's functions. The Green's functions are discussed in Appendix B of this paper. Suffice it to say that they are linearly independent solutions to the equation

$$\frac{d^2}{dr^2} G_i^{(\frac{1}{2})}(|k_i|r) + [\pm(|k_i|)^2 + \frac{2(NZ-NE)}{r} - \frac{\ell_i(\ell_i+1)}{r^2}]$$

$$G_i^{(\frac{1}{2})}(|k_i|r) = 0 \qquad (5.10)$$

satisfying the Wronskian relation (insuring linear independence).

$$[\frac{d}{dr} G_i^{(1)}(|k_i|r)] G_i^{(2)}(|k_i|r) - G_i^{(1)}(|k_j|r)$$

$$[\frac{d}{dr} G_i^{(2)}(|k_i|r)] = 1 \qquad (5.11)$$

At this point we expand the solution to (5.8)

$$\psi_{ik}(r) = \psi_{ik}^{(0)}(r) + \sum_{m,\alpha_m} \psi_{im}^{(\alpha_m)}(r)\, C_{mk}^{(\alpha_m)} \qquad (5.12)$$

Thus

$$\begin{aligned}\psi_{ik}^{(\alpha)}(r) = {} & \delta_{\alpha o}\,\delta_{ik}\, G_i^{(1)}(|k_i|r) + \int_o^r dx\, G_i^{(2,1)}(r|x) \\ & \Big[\sum_n V_{in}(x)\,\psi_{nk}^{(\alpha)}(x) \\ & + \sum_{\alpha_i}{}' B_i^{(\alpha_i)} P_{\rho_n}(x)\Big\{\frac{1}{x^{t+1}}\int_o^x dy\, P_{\rho_i}(y)\, \psi_{nk}^{(\alpha)}(y)\, y^{t-x^t} \\ & \int_o^x dy\, P_{\rho_i}(y)\,\psi_{nk}^{(\alpha)}(y)\, y^{-(t+1)}\Big\}\Big] \\ & + \delta_{ik}\, B_k^{(\alpha)} \int_o^r dx\, G_k^{(2,1)}(r|x)\, D_m^{(\alpha)}(x)\, dx\end{aligned} \qquad (5.13)$$

where

$$C_{mk}^{(\alpha_i)} = \begin{cases} \displaystyle\int_o^\infty dy\, y^{-(t+1)} P_{\rho_m}(y)\,\psi_{nk}(y) & \alpha_i = 1,2,\ldots,NEX(i) \\ \displaystyle\sum_{\zeta,n} E_\zeta^\nu \int_o^\infty dy\, V_{\zeta n}(y)\,\psi_{nk}(y) & \alpha_i = NEX(i)+1,\ldots,NEX(i)+NV \\ M_\lambda^{mk}\,\delta_{\ell_m \ell_\lambda} & \alpha_i = NEX(i)+NV+1,\ldots, \\ & \quad NEX(i)+NV+NOTH(i) \end{cases} \qquad (5.14)$$

and

$$B_i^{(\alpha)} = \begin{cases} 0 & ; \quad \alpha = 0 \\ B^{(\alpha_i)} & ; \quad \alpha = \alpha_i = 1,2,\ldots,NEX(i) \\ 1 & ; \quad \alpha = NEX(i)+1,\ldots \end{cases} \tag{5.15}$$

$$D_i^{(\alpha)} = \begin{cases} 0 & ; \quad \alpha = 0 \\ P_{\rho_n}(x)x^t & ; \quad \alpha = \alpha_i = 1,2,\ldots,NEX(i) \\ V_{\nu_i}(x) & ; \quad \alpha = \alpha_i = NEX(i)+1,\ldots,NEX(i)+NV \\ P_\lambda(x) & ; \quad \alpha = \alpha_i = NEX(i)+NV+1,\ldots, \\ & \qquad\qquad NEX(i)+NV+NOTH(i) \end{cases} \tag{5.16}$$

The M_λ^{mk} are determined by the constraint condition

$$\delta_{\ell_m \ell_\lambda} \int_0^\infty dx\ P_\lambda(x)\psi_{mk}(x) = 0 \tag{5.17}$$

A critical part of the utility of NIIEM is the fact that the C-coefficients are not determined until after the equations for the $\psi^{(\alpha)}$'s have converged. The C-coefficients are then determined by solving the set of simultaneous equations

$$\Delta_{\alpha_i} C_{ij}^{(\alpha_i)} = D_{ij}^{(\alpha_i,0)} + \sum_{m,\beta_m} D_{im}^{(\alpha_i,\beta_m)} C_{mj}^{(\beta_m)} \qquad (5.18)$$

where

$$D_{ij}^{(\alpha_i,\beta)} = \int_0^\infty dy\, E_i^{(\alpha_i)}(y)\psi_{nk}^{(\beta)}(y) \quad ; \quad \beta = \{0,\beta_j\} \qquad (5.19)$$

and

$$E_i^{(\alpha_i)}(r) = \begin{cases} P_{\rho_i}(r)/r^{t+1} & ; \ \alpha_i = 1,\ldots,NEX(i) \\ \sum_n [\sum_\zeta E_{\zeta n} V_{\zeta n}] & ; \ \alpha_i = NEX(i)+1,\ldots, \\ & \qquad NEX(i)+NV \\ P_\lambda(r) & ; \ \alpha_i = NEX(i)+NV+1,\ldots, \\ & \qquad NEX(i)+NV+NOTH(i) \end{cases} \qquad (5.20)$$

Thus we see that the Eq. (5.13) for the particular solutions only contain integrals from $0 \to r$ and not also $r \to \infty$. It then appears that, even with exchange terms included, we may begin the integration process at the origin, integrate out to the frame transformation point r_t, perform the transformation, and continue the integration to infinity where we determine the C-coefficients and then the R-matrix elements. Note that in this paper,

only exchange terms are considered, and no correlation or orthogonality terms are considered.

One of the techniques of solving the close-coupling equations involves dropping the exchange terms after they have converged. This eliminates the necessity for integrating the particular solutions all the way to infinity; only the homogeneous solution needs to be integrated to infinity. In the context of the frame transformation theory, this makes for the possibility that the transformation may be performed before exchange terms are dropped, or after exchange terms are dropped. If the transformation is performed before exchange is dropped, the C-coefficients must also be transformed. Thus, from (5.22)

$$\underline{FL}^{(0)} + \sum_{\alpha_m} \underline{FL}^{(\alpha_m)} \underline{CL}^{(\alpha_m)} = \underline{Z}^{-1} \underline{U}^{-1} [\underline{FB}^{(0)} + \sum_{\alpha_m} \underline{FB}^{(\alpha_m)} \underline{CB}^{(\alpha_m)}] \underline{Z} \tag{5.21}$$

$$= \underline{Z}^{-1} [\underline{U}^{-1} \underline{FB}^{(0)}] \underline{Z} + \sum_{\alpha_m} Z^{-1} (\underline{U}^{-1} \underline{FB}^{(\alpha_m)}) \underline{Z} \underline{Z}^{-1} \underline{CB}^{(\alpha_m)} Z \tag{5.22}$$

Now from (5.13) we can write

$$\underline{FB}^{(\alpha_m)} = -\underline{GB}^{(1)}(\underline{k}r)^{(2)}\underline{HB}^{(\alpha_m)} + \underline{GB}^{(2)}(\underline{k}r)^{(1)}\underline{HB}^{(\alpha_m)}(r) \tag{5.23}$$

Consistent with the approximation suggested by Chang and Fano,[11] we assume

$$\underline{GL}^{(\frac{1}{2})}(\underline{k}r_t) = \underline{GB}^{(\frac{1}{2})}(\underline{k}r_t) \tag{5.24}$$

Thus

$$^{(\frac{1}{2})}\underline{HL}^{(0)}(r) = \underline{Z}^{-1}[\underline{U}^{-1}\,^{(\frac{1}{2})}\underline{HB}^{(0)}]\,\underline{Z}$$

$$^{(\frac{1}{2})}\underline{HL}^{(\alpha_m)}(r) = \underline{Z}^{-1}[\underline{U}^{-1}\,^{(\frac{1}{2})}\underline{HB}^{(\alpha_m)}]\,\underline{Z}$$

$$\underline{CL}^{(\alpha_m)} = \underline{Z}^{-1}\,\underline{CB}^{(\alpha_m)}\,\underline{Z} \tag{5.25}$$

For the case in which the transformation is performed after the exchange is dropped, the transformation reduces to that of the homogeneous solutions, $^{(\frac{1}{2})}\underline{HL}^{(0)}(r)$.

CHAPTER VI

e^--H_2 SCATTERING RESULTS

A. Rotational Frame Transformation Criteria

It is the objective of this section to describe semi-quantitative frame transformation criteria for the e^--H_2 scattering problem. Truncation of the system wave function expansion results in a finite set of close-coupling problems (partial waves). The frame transformation point must be established for each partial wave and in general may also depend on the energy of the incident electron. Essentially three things must be considered in fixing the transformation point: the direct potential matrix elements, the rotational matrix elements, and the projectile energy. It would be desirable to vary the transformation point (r_t) according, also, to the projectile angular momentum quantum number; however, this is not possible because the radial functions describing the projectile motion are coupled and must all be determined simultaneously at any point which might be used as r_t.

The maximum value that r_t may assume is fixed for each partial wave by comparing the rotational matrix elements, VR_{ij}, in each channel with the direct potential matrix elements, VD_{ij}, in each channel, within the set of coupled equations describing a particular partial wave in the body frame. From the origin to the maximum value of

r_t, $VD_{ij} >> VR_{ij}$. This is the motivation for neglecting the rotational potential in the body frame. As soon as any one of the direct potential matrix elements decreases in magnitude, as a function of r, so as to be comparable to the rotational matrix element which is neglected, the body frame equations lose their validity. This establishes $(r_t)_{max}$.

Finally, the projectile energy, E, must be considered to fix r_t such that $0 \leq r_t \leq (r_t)_{max}$. It is this consideration that introduces much of the qualitative characteristic of the choice of r_t. In performing the frame transformation, the approximation explicitly defined by Eq. (4.24) is used; that is, the body-frame Green's function matrix is equal to the lab-frame Green's function matrix. This of course means that the individual matrix elements are assumed equal. Initially one might think that this fixes r_t to be the point where the lab frame Green's functions cross the body-frame Green's functions. This is of little help since the open and closed channel functions cross at different points and indeed, each matrix element intersection point is in general different. We are then forced to turn to examination of certain qualitative criteria.

In general terms, the validity of the body frame approach depends on the fact that the projectile energy is much greater than the energy of molecular rotation. This only requires energies greater than 10^{-4} eV. We thus

conclude that at zero energy, the lab-frame is applicable. However, because of the practical necessity of the truncation of the close-coupling expansion, this does not necessarily mean that the body frame is applicable at higher energies. To be sure that the body-frame is absolutely more applicable at all r-values, the projectile energy should be well above all included excitation thresholds. The onset of confidence then for applicability of the body frame for $r<(r_t)_{max}$ might be the dissociation energy for the particular electronic state considered. Thus for energies greater than or equal to the dissociation energy, D_o, the body frame is applicable for $r \geq (r_t)_{max}$.

An interesting aspect of the $e^- - H_2$ encounter was demonstrated by Gerjuoy and Stein[30] in 1955 by analyzing the collision cross section just above the rotational excitation threshold. They showed that at these energies the cross section is determined solely by the electron-quadrapole interaction which goes as $-Q/r^3$ and is very long range. We thus conclude that just above excitation thresholds, the lab-frame is absolutely more applicable than the body-frame. On the basis of these qualitative considerations, we propose to define the transformation point, r_t, via a functional relationship:

$$r_t = \begin{cases} (r_t)_{max} \sin\left[\left(\frac{\pi}{2}\right)\left(\frac{E-E_t}{D_o-E_t}\right)\right] & ; \quad E \leq D_o \\ (r_t)_{max} & ; \quad 10eV \geq E > D_o \end{cases} \tag{6.1}$$

where E is the incident electron energy, E_t is the nearest excitation threshold, D_o is the dissociation energy, and $(r_t)_{max}$ is the maximum value of the transformation point fixed by comparing the rotational potential matrix elements and the direct potential matrix elements. On the basis of this definition of the transformation point, we proceed to describe the results of calculations.

B. e^--H_2 Scattering Below 100 meV

There has been recent experimental interest in the extremely low energy region of the e^--H_2 encounter generated by the observation of certain structures in the total cross section below 100 meV. This energy region contains the first three rotational levels of H_2 located as shown in Figure 7. In the top part of the figure, the relative transmitted electron count taken with a time-of-flight spectrometer, by Raith and Land[14] is illustrated. They offer these results as evidence for what they describe as resonances in the total e^--H_2 cross section at 24 and 70 meV. Previous experiments by Crompton and Robertson[31] had detected similar anomalies in electron swarm experiments at high H_2 pressures and low energies. Crompton and Robertson concluded that their data supported an hypothesis put forward earlier by Frommhold[32] that the structures resulted from a rotationally-excited auto-ionizing state of H_2^-. As pointed out by Raith and Land,[14]

this is in contradiction to the theoretical belief that the ground state of H_2^- is $^2\Sigma_u^+$ and located at approximately 2.5 eV. In addition it is known that Henry and Lane[17] detected no such closed-channel resonances. Other suggestions that the structures are due to pressure effects have also been published by Legler.[33]

Raith and Land conclude that because of the low H_2 gas pressure used in their experiment, 10^{-3} Torr, the low energy cross section structures are due to single e^--H_2 encounters rather than pressure effects. As to the exact cause, they don't speculate.

In the lower part of Figure 7, the total e^--H_2 cross section is given as a function of projectile energy. Curve B is the total cross section for scattering from the v=0, j=0 ground state and curve C is the total cross section for scattering from the v=0, j=1 ground state. In this energy region the total cross section is dominated by the elastic cross sections $\sigma([v=0, j=0] \rightarrow [v=0, j=0])$ and $\sigma([v=0, j=1] \rightarrow [v=0, j=1])$. One of the interesting characteristics of H_2 gas is the fact that it is essentially a mixture of para H_2 and ortho H_2 with virtually no transitions between the two states. Additionally, the ground state energy of ortho H_2 is greater than for para H_2 as well as is the statistical weight (9:1). The H_2 gas used by Raith and Land[14] was just such a mixture of ortho and para H_2. It is then interesting that the first

structure illustrated in Figure 7 is just above the ground state of ortho H_2 (~15 meV) at approximately 24 meV. Although the present calculation offers no indication as to the physical explanation of this particular structure at 24 meV, it appears to be associated with the energetically allowed quantum mechanical elastic scattering process $\sigma([v=0, j=1] \rightarrow [v=0, j=1])$. The detailed physical explanation might be indicated by the result of a similar experiment on para H_2 which has been separated from ortho H_2. If the structure at 24 meV is not observed for e^--(para H_2) scattering, it would then be interesting to analyze the details of the encounter of a 0→15 meV (referred to the ground state of para H_2) electron with the statistically abundant ortho H_2 in a ortho-para mixture.

There is a second structure in Figure 7 located at approximately 70 meV. Although the contribution to the total cross section of the partial wave characterized by total angular momentum, two, and parity, plus one, is small, a detailed look at its contribution is instructive in interpreting this second structure. In Figure 8 Curve A is the elastic cross section $\sigma([v=0, j=0] \rightarrow [v=0, j=0])$ for the partial wave under consideration $J=0$, $\pi=+1$. In this particular partial wave, we have included electron s, p, d waves. Included in the close-coupling expansion are the rotational states j=0, 2 as well as the vibrational states v=0, 1. Curve B is then the cross section

$\sigma([v=0, j=0] \rightarrow [v=0, j=2])$. Curve C is the same cross section with a particular set of channels left out $(v\ell j) = (002), (102)$. Thus Curve B exhibits a structure that resembles a shape resonance. However, the contribution to the total cross section is negligible as can be seen in Figure 7. By observing the fact that Curve C does not exhibit this characteristic shape, it is concluded that for J=2, the $(v\ell j) = (002)$ channel is responsible for the observed effect.

C. Pure Rotational Excitation, 0→10 eV

In Figure 9, the cross section corresponding to the process $(v=0, j=1 \rightarrow 3)$ is presented. Curve A results when the transformation point is $r_t=0$. Curve B results when the transformation is performed at $r_t=1.5\ a_o$. Curve C results when the transformation is performed at $r_t=7.0\ a_o$ which is slightly beyond the $(r_t)_{max} \sim 6.0\ a_o$. Finally, Curve D is the curve resulting from the use of a dynamic transformation point, with energy variation defined by (6.1). For this particular excitation process there is a chance to compare with the experimental result of Ehrhardt and Linder.[35]

The smallest cross section resulted from a transformation point just outside the molecular electron cloud at $1.5\ a_o$. As the transformation point is moved past $1.4\ a_o$, the cross section starts to rise back toward the lab frame

result, but doesn't quite reach it (see Table 2). Thus the overall effect of using a variable transformation is to lower the cross section toward the experiment. One thing to note is that the cross section peaks don't significantly vary. As a result, the dynamic transformation cross section peaks in approximately the same place and doesn't shift to higher energies as the experiment indicates. Thus, the magnitude of the cross section is significantly improved with respect to the experiment, although the shape is approximately the same.

In Figure 10 and Table 3, the cross section for the process (v=0, j=0→2) is given. The correspondence between the transformation points and the curves is the same as in Figure 9. We notice for this process, the cross section resulting from transforming at r_t=7.0 is higher than the lab frame result. The effect is to raise the cross section in the dynamic frame transformation case, above the lab frame result for energies greater than 7 eV. There are no experimental results above 1 eV for this cross section. The agreement below 1 eV is as expected from the fact that the lab frame result of Henry and Lane[17] essentially, by (6.1) is the same as the present calculation.

D. Vibrational Excitation Cross Sections, 0→10 eV

We are unable to establish $(r_t)_{max}$ for vibrational transformations, as we did above for rotational transformations, because the vibrational potential matrix elements depend on an integral over the internuclear separation magnitude, containing the scattering function for the impacting electron. We can, however, estimate it, as Henry and Chang did, to be at 5.0 a_o. Using this value for $(r_t)_{max}$, in formula (6.1), we proceed to describe the results of the calculations involved in determining the total cross section for the vibrational excitation process, v=0 1.

In Figure 11, we give several results for the cross section $\sigma([v=0, j=1] \rightarrow [v=1, j=1])$. Curve A is the result obtained using $r_t=0$ for all electron energies. Curve B results from using $r_t=1.4$ a_o for all energies and Curve C is the result of the dynamic frame transformation. As you notice, Curve B has a resonance spire located at 1.05 eV. It then descends to a local minimum of approximately $0.35*10^{-16}$ cm^2 at 1.45 eV and then rises to a local maximum of approximately $0.5x10^{-16}$ cm^2 at 2.65 eV. The spire is a nonphysical result indicating that the transformation point of 1.4 a_o is not appropriate for an energy less than about 1.45 eV. The initial appearance of this spire is first seen as the transformation point

reaches 0.8 a_o as it is moved out from the origin. As the transformation passes 2.4 a_o, the spire disappears. Thus it is obviously associated with the points on which the vibrational wave functions are tabulated; eg. the vibrational wave functions are tabulated on the grid s=0.8, 1.2, 1.4, 1.6, 2.0, and 2.4 a_o. The spire first appears, as r_t is moved out from the origin, at an energy of approximately 0.6 eV, just above the v=0, j=1 threshold. Its energy position then migrates to about 1.05 eV at r_t=1.4 a_o. The movement then continues with the top of the spire decreasing in height and finally disappears at 2.4 a_o leaving a smooth cross section. The local maximum located above the spire in energy, decays from the r_t=0 result, to its least value at r_t=1.4 a_o. It then starts to rise again to its approximately final value when r_t=2.4 a_o. For r_t values less than 0.8 a_o and greater than 2.4 a_o, the cross section changes insignificantly. We note that this spire appears only for ortho hydrogen and not in para hydrogen.

In Figure 12, we give similar results for the simultaneous rotational-vibrational cross section $\sigma([v=0, j=1]\rightarrow[v=1, j=3])$. The letters describing the curves have the same meaning as in Figure 11. Again we see that anomalous resonance spire and note that the behavior is quite similar to that described above. We emphasize that these are anomalous structures and don't

appear when the dynamic frame transformation is correctly used.

The cross sections for the excitation processes for para hydrogen are given in Tables 6-8. In these cases, the curves change smoothly as r_t moves from 0→5 a_o.

Finally, in Figure 13, the result of the present calculation of the total vibrational cross section (statistically weighted) v=0→1 is presented in Curve A. Curve B gives Henry's[6] lab frame result and Curve C gives Henry and Chang's[12] fixed nuclei result. Also, two experiments are given for comparison. The peak of our result is at about 2.7 eV and falls between the two other theoretical results. It is however higher than both experiments. The agreement between the Ehrhardt et al. experiment, the fixed nuclei calculation, and the present result above 4.5 eV, is satisfactory. However, below 4.5 eV, there is significant disagreement in magnitude and shape among all the results. Because of the somewhat arbitrary choice of transformation formula 6.1, we are not prepared to make a conclusive statement for energies less than 4.5 eV.

The present work has demonstrated the use of the dynamic frame transformation theory in calculating cross sections for electrically excited nuclear transitions in H_2. The work may readily be extended to other homonuclear diatomic molecules such as N_2. However, there seems to be

a significant problem with the shapes of the cross sections between 0.5 eV and 4.5 eV. In order to produce results that can be stated with more confidence, the next step is to put in the first excited electronic state instead of the polarization potential. In short, follow the line of development that close coupling theory has taken in application to electron atom collisions.

BIBLIOGRAPHY

1. B. R. Judd, Operator Techniques in Atomic Spectroscopy, (New York: McGraw-Hill Book Company, Inc., 1963), pp. 2-6.
2. D. S. Urch, Orbitals and Symmetry (Harmondsworth, Middlesex, England: Penguin Books, Ltd., 1970), pp. 53-56.
3. K. Smith, The Calculation of Atomic Collision Processes, (New York: Wiley-Interscience, 1971), pp. 96-107.
4. G. Herzberg, Spectra of Diatomic Molecules, (New York: Van Nostrand Reinhold Co., 1950).
5. F. Linder, in Proceedings of the Sixth International Conference on the Physics of Electronic and Atomic Collisions (MIT Press, Cambridge, Mass., 1969), p. 141.
6. R. J. W. Henry, Phys. Rev. A2, 1349 (1970).
7. A. M. Arthurs, A. Dalgarno, Proc. Roy. Soc. A256, 540 (1960).
8. R. W. B. Ardill, W. D. Davison, Proc. Roy. Soc. A304, 465 (1968).
9. N. F. Lane, R. J. W. Henry, Phys. Rev. 173, 183 (1968).
10. D. E. Golden, N. F. Lane, A. Temkin, E. Gerjuoy, Rev. Mod. Phys. 43, 642 (1971).
11. E. S. Chang, U. Fano, Phys. Rev. A6, 173 (1972).

12. R. J. W. Henry, E. S. Chang, Phys. Rev. A5, 276 (1972).

13. L. Frommhold, Phys. Rev. 172, 118 (1968).

14. W. Raith, J. E. Land, "Further Evidence for Existence of the Frommhold Resonances in e-H_2 Scattering Below 100 meV", in Proceedings of the Third International Conference on Atomic Physics, 1972, University of Colorado, Boulder.

15. H. A. Bethe, R. Jackiw, Intermediate Quantum Mechanics, (New York: W. A. Benjamin, Inc., 1968), pp. 177-186.

16. M. Born, J. R. Oppenheimer, Ann. Physik 84, 457 (1927).

17. R. J. W. Henry, N. F. Lane, Phys. Rev. 183, 221 (1969).

18. S. Huzinaga, Prog. Theoretical Phys. 17, 162 (1957).

19. S. C. Wang, Phys. Rev. 31, 579 (1928).

20. U. Fano, Phys. Rev. A2, 353 (1970).

21. D. M. Brink, G. R. Satchler, Angular Momentum, (Oxford, England: Oxford University Press, 1968), pp. 19-27.

22. E. R. Smith, R. J. W. Henry, Phys. Rev. A1, 1585 (1973).

23. C. A. Weatherford, R. J. W. Henry, M. C. Bruels, Journal of the Academy of Sciences of India (to be published).

24. V. D. Obedkov, Optics and Spectros 17, 101 (1964).

25. S. Hara, J. Phys. Soc. Japan 27, 1262 (1969).

26. J. C. Browne, private communication.

27. F. Linder, H. Schmidt, Z. Naturforsch 269, 1603 (1971).

28. M. Abramowtiz, I. A. Stegun, Handbook of Mathematical Functions (Dover Publ., Inc., New York, 1965).

29. E. T. Whittaker, G. N. Watson, A Course of Modern Analysis, (Cambridge, England: Cambridge University Press, 1965).

30. E. Gerjuoy and S. Stein, Phys. Rev. 97, 1671 (1955).

31. R. W. Crompton and A. G. Robertson, Austral. J. Phys. 24, 543 (1971).

32. L. Frommhold, Phys. Rev. 172, 118 (1968).

33. W. Legler, Phys. Lett. 31A, 129 (1970).

34. P. G. Burke, A. Joanna Taylor, J. Phys. B. 2, 44 (1969).

35. H. Ehrhardt and F. Linder, Phys. Rev. Letters 21, 419 (1968).

36. H. Ehrhardt, L. Langhans, F. Linder, H. S. Taylor, Phys. Rev. 173, 222 (1968).

37. G. J. Schulz, Phys. Rev. 135, A988 (1964).

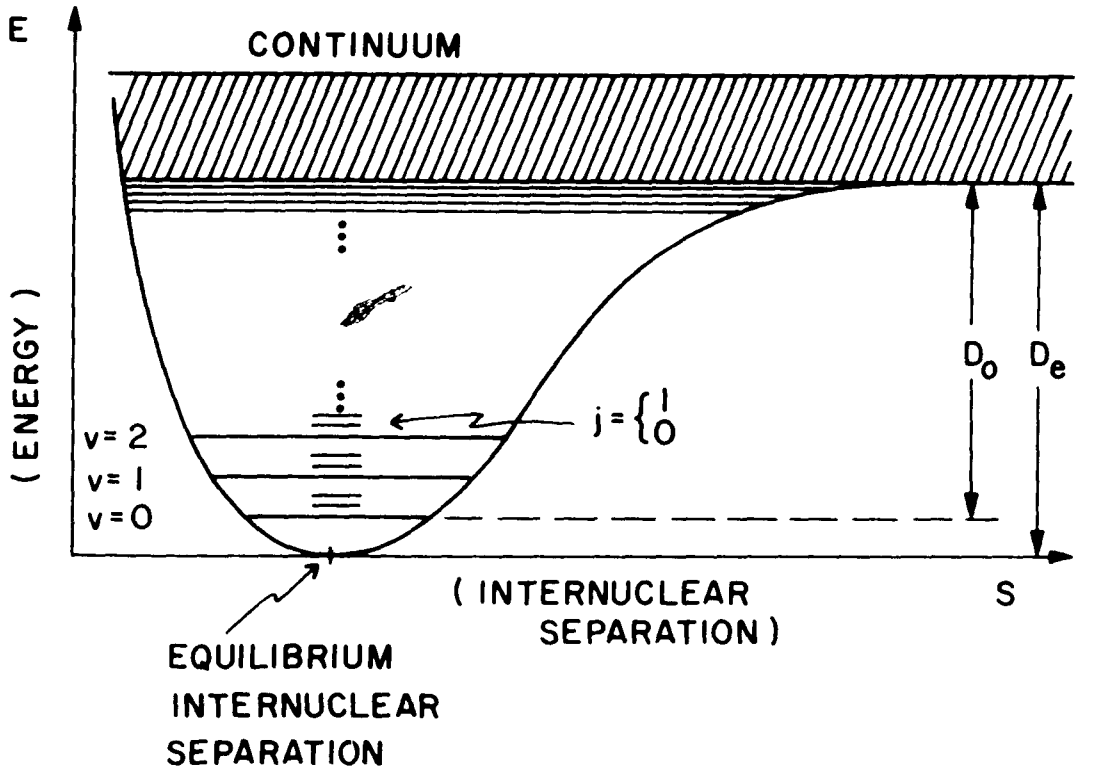

j = ROTATIONAL QUANTUM NUMBER
v = VIBRATIONAL QUANTUM NUMBER
D_o = DISSOCIATION ENERGY
D_e = BINDING ENERGY

Figure 1

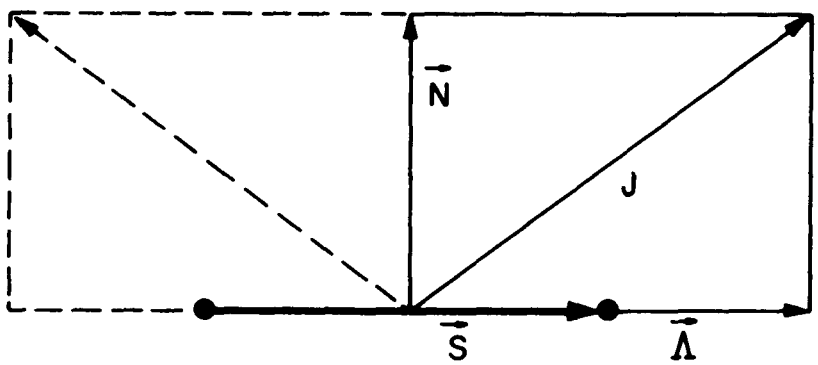

Figure 2a

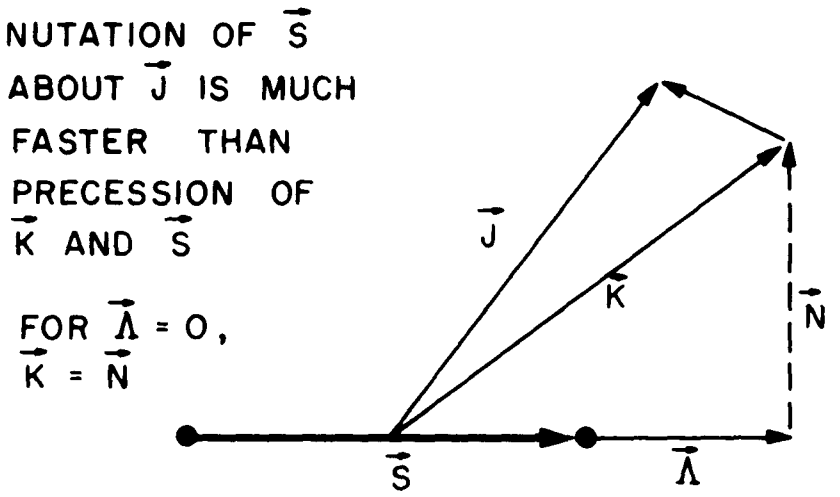
NUTATION OF $\vec{S}$
ABOUT $\vec{J}$ IS MUCH
FASTER THAN
PRECESSION OF
$\vec{K}$ AND $\vec{S}$
FOR $\vec{\Lambda} = 0$,
$\vec{K} = \vec{N}$
$\vec{J}$
$\vec{K}$
$\vec{N}$
$\vec{S}$
$\vec{\Lambda}$

Figure 2b

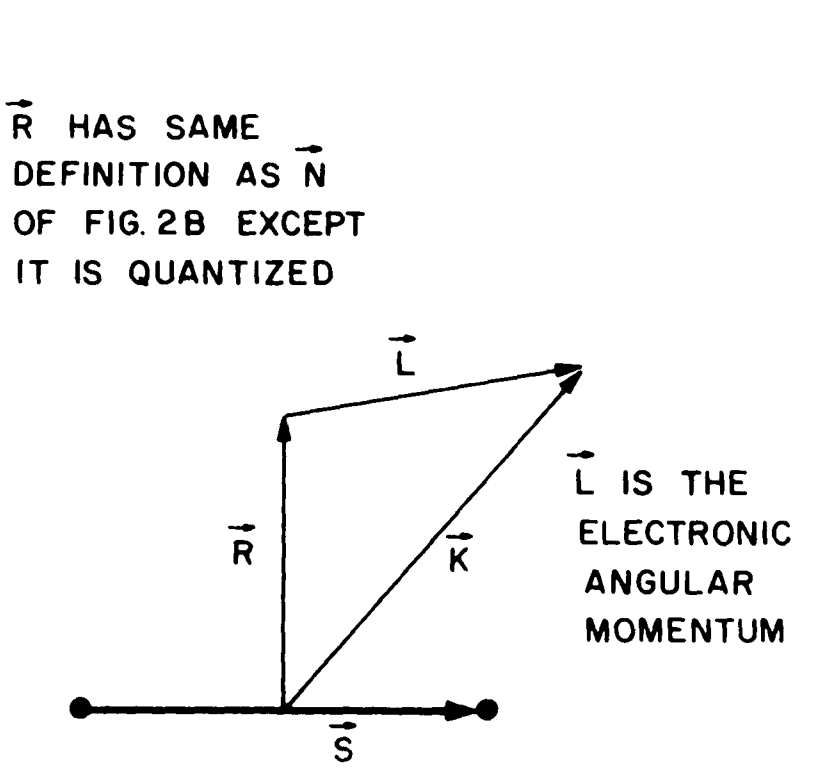
$\vec{R}$ HAS SAME
DEFINITION AS $\vec{N}$
OF FIG. 2B EXCEPT
IT IS QUANTIZED
$\vec{L}$
$\vec{R}$
$\vec{K}$
$\vec{S}$
$\vec{L}$ IS THE
ELECTRONIC
ANGULAR
MOMENTUM

Figure 2c

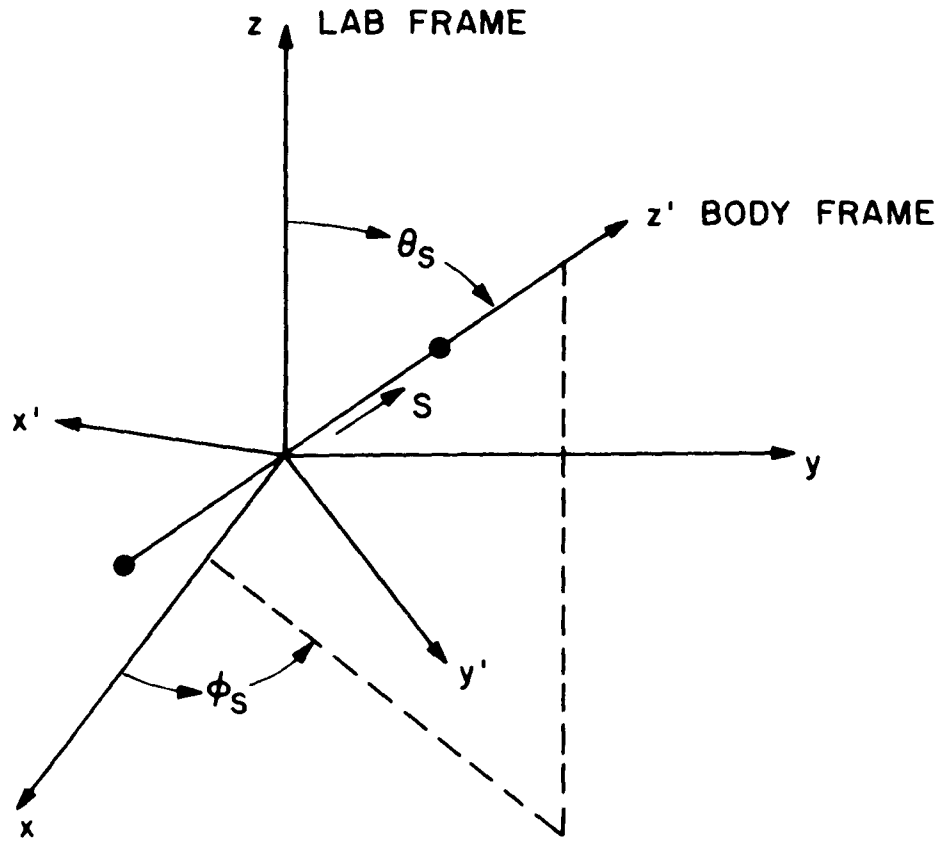

Figure 3

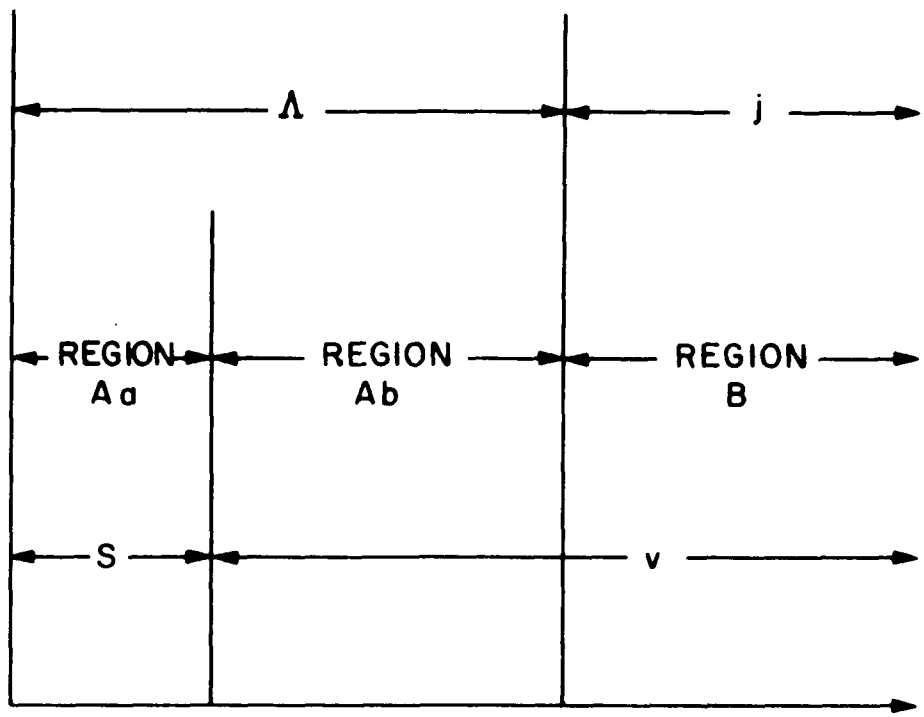

Figure 4

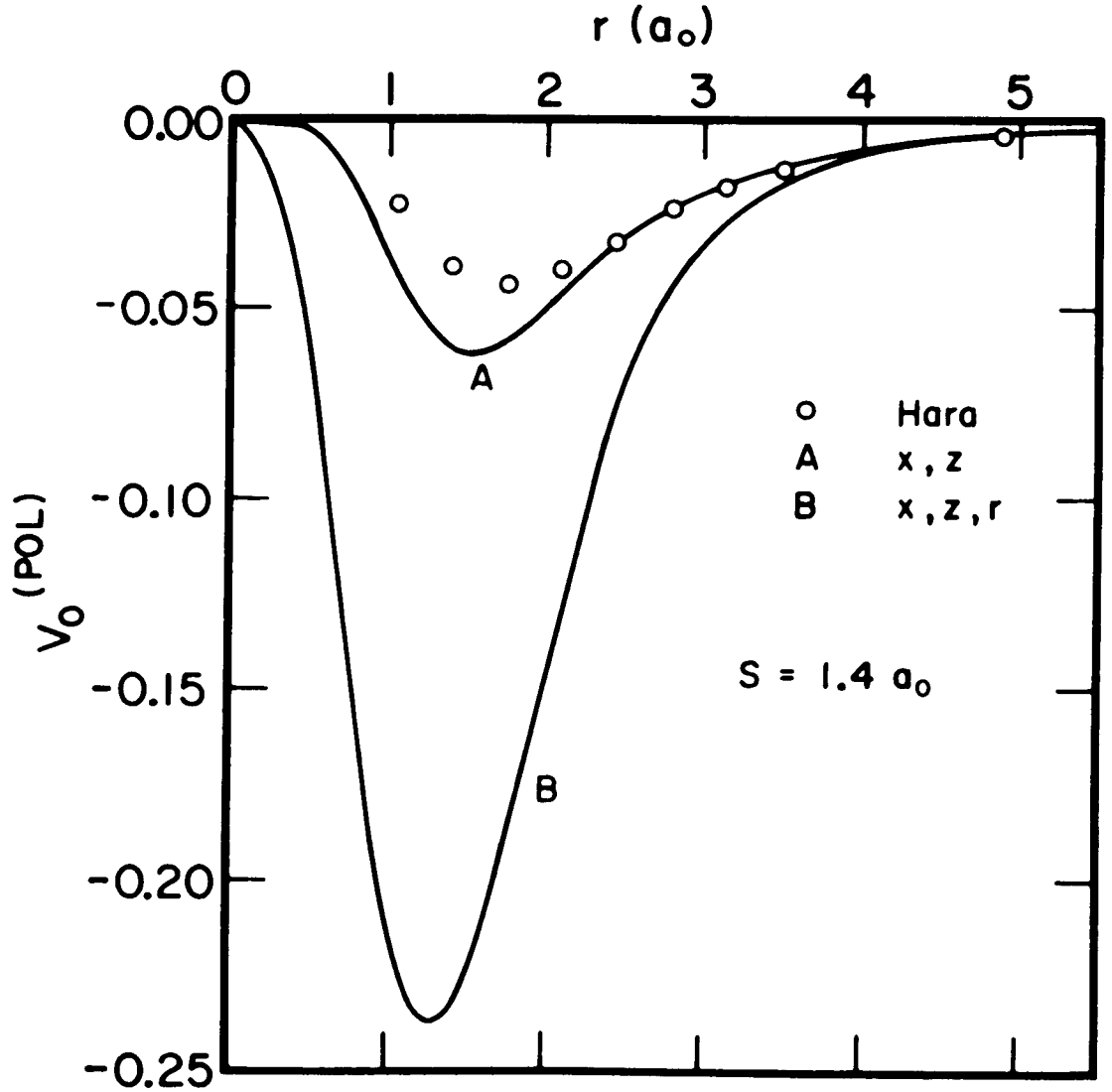
r (a₀)
0
1
2
3
4
5
0.00
-0.05
-0.10
-0.15
-0.20
-0.25
V₀ (POL)
A
B
o Hara
A x, z
B x, z, r
S = 1.4 a₀

Figure 5

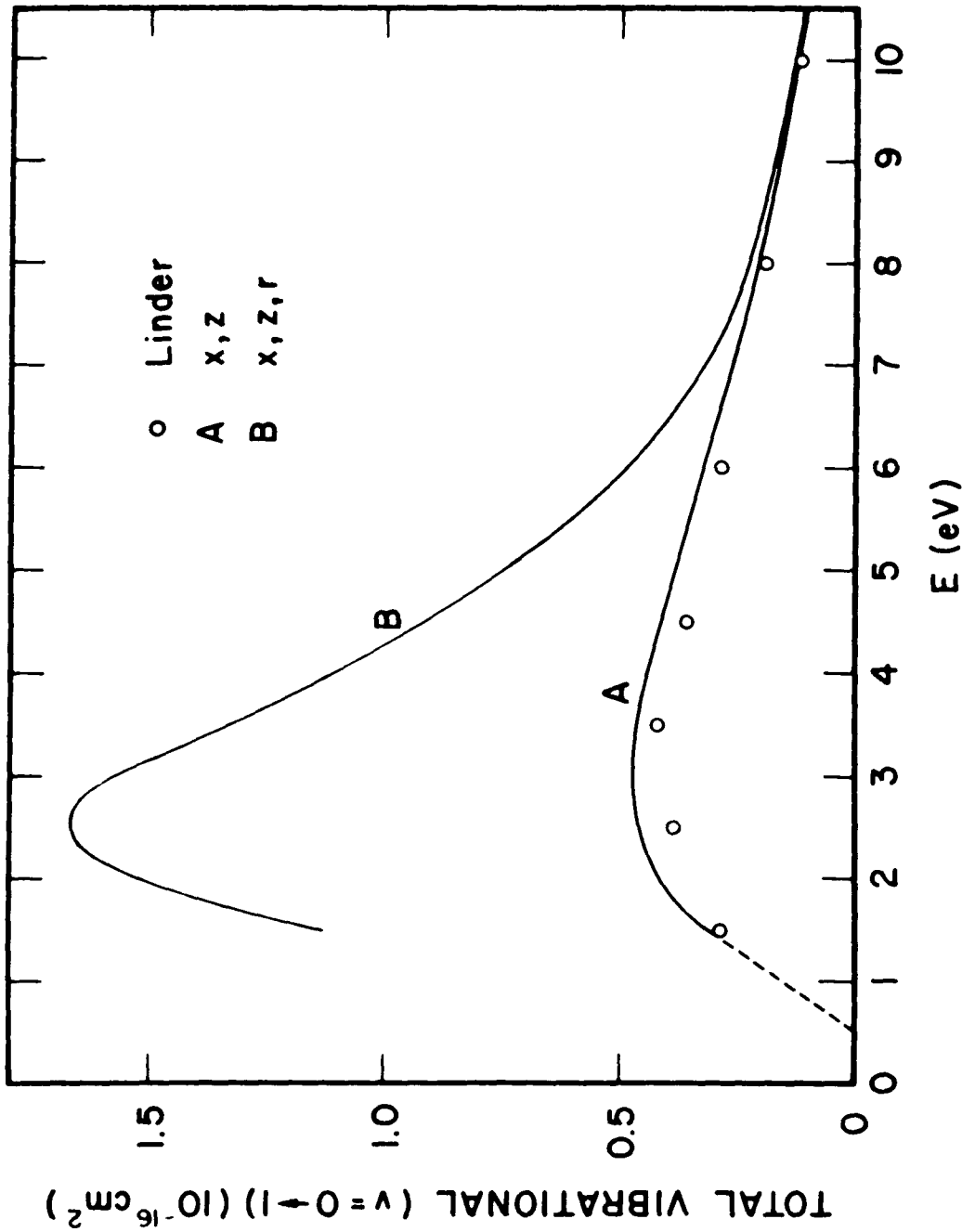
o Linder
A x,z
B x,z,r
A
B
0
1
2
3
4
5
6
7
8
9
10
E (eV)
0
0.5
1.0
1.5
TOTAL VIBRATIONAL (v = 0 → 1) (10⁻¹⁶ cm²)

Figure 6

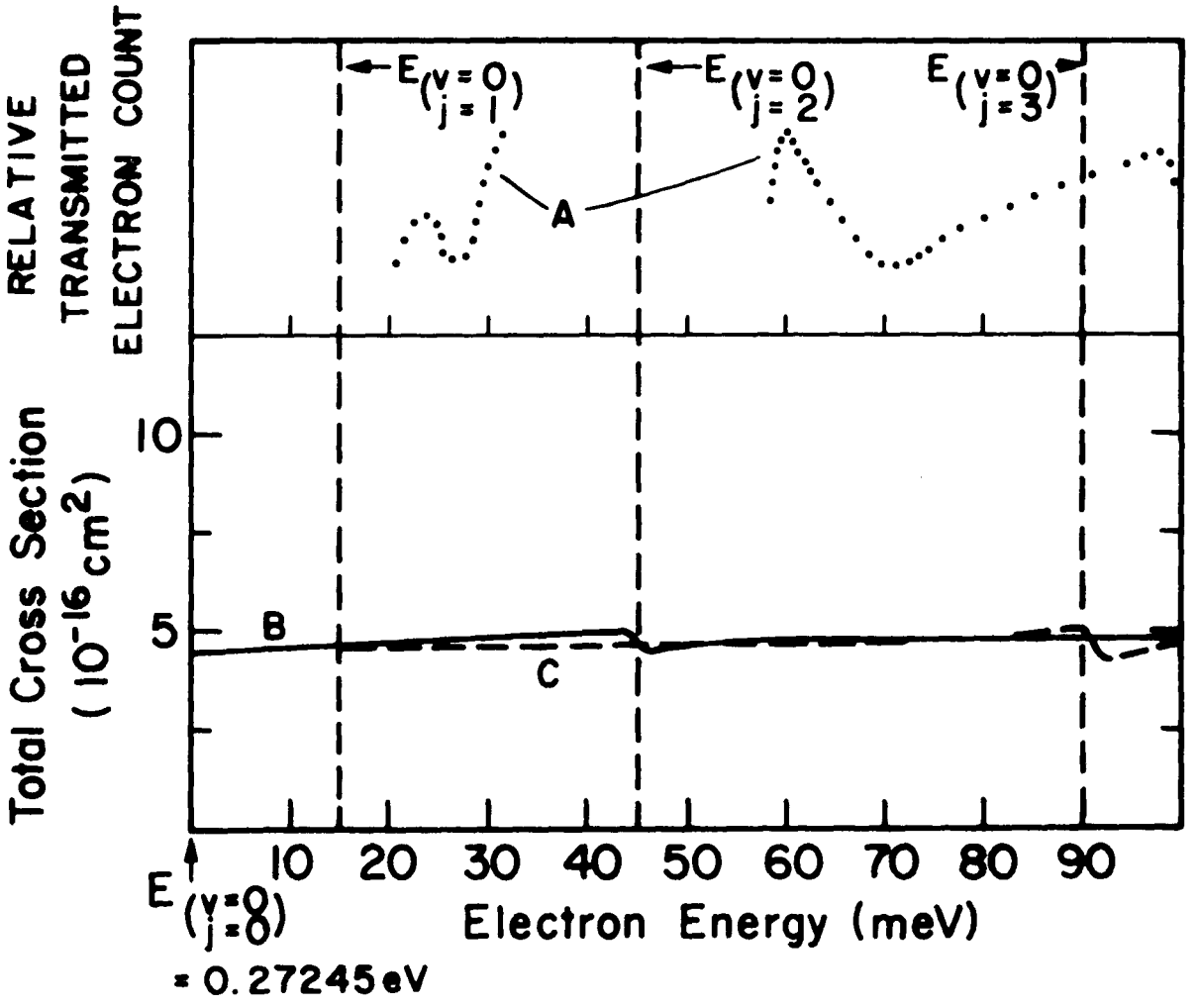
RELATIVE TRANSMITTED ELECTRON COUNT
E(v=0, j=1)
E(v=0, j=2)
E(v=0, j=3)
A
B
C
Total Cross Section (10^-16 cm^2)
10
5
10 20 30 40 50 60 70 80 90
E(v=0, j=0) = 0.27245 eV
Electron Energy (meV)

Figure 7

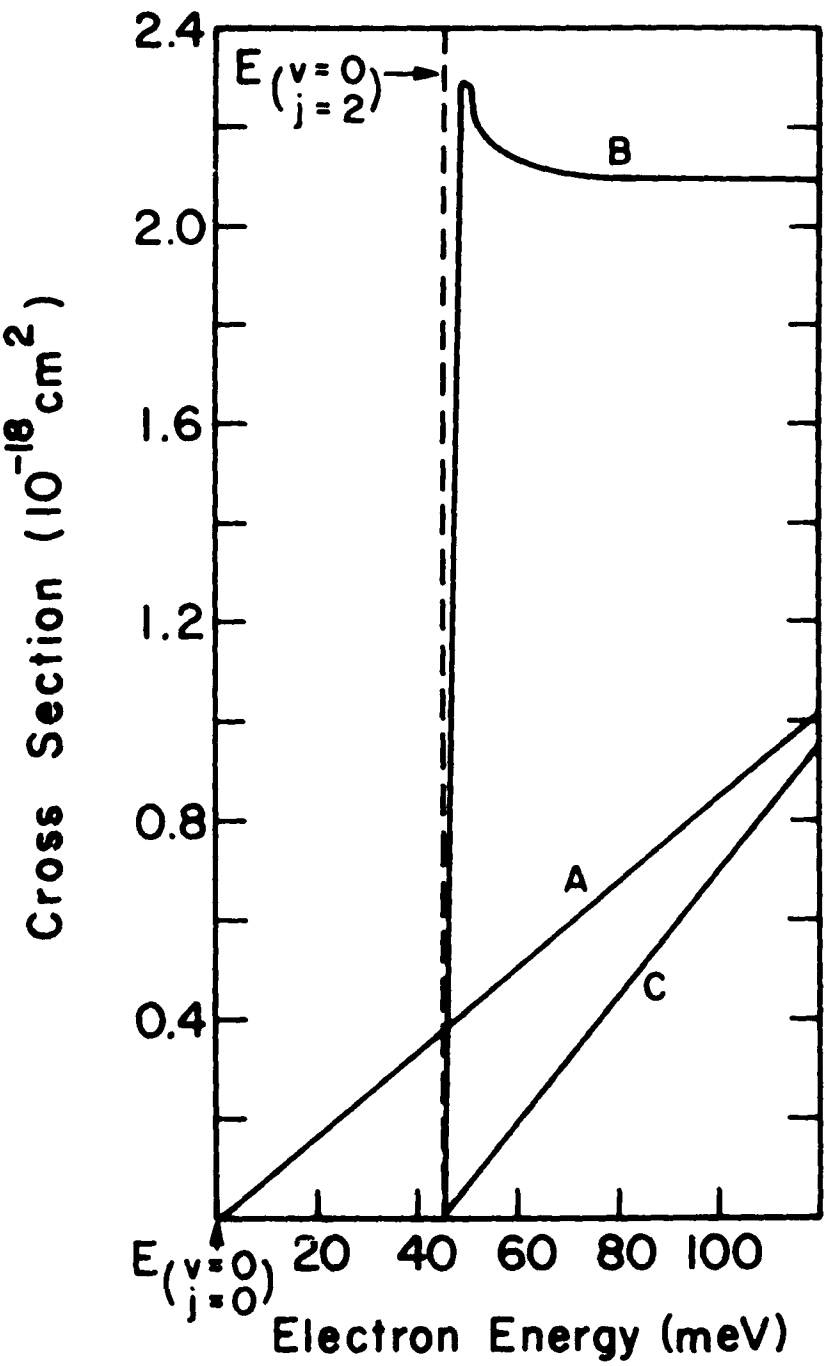
2.4
2.0
1.6
1.2
0.8
0.4
E(v=0, j=2)
B
A
C
E(v=0, j=0)
20
40
60
80
100
Cross Section (10^-18 cm^2)
Electron Energy (meV)

Figure 8

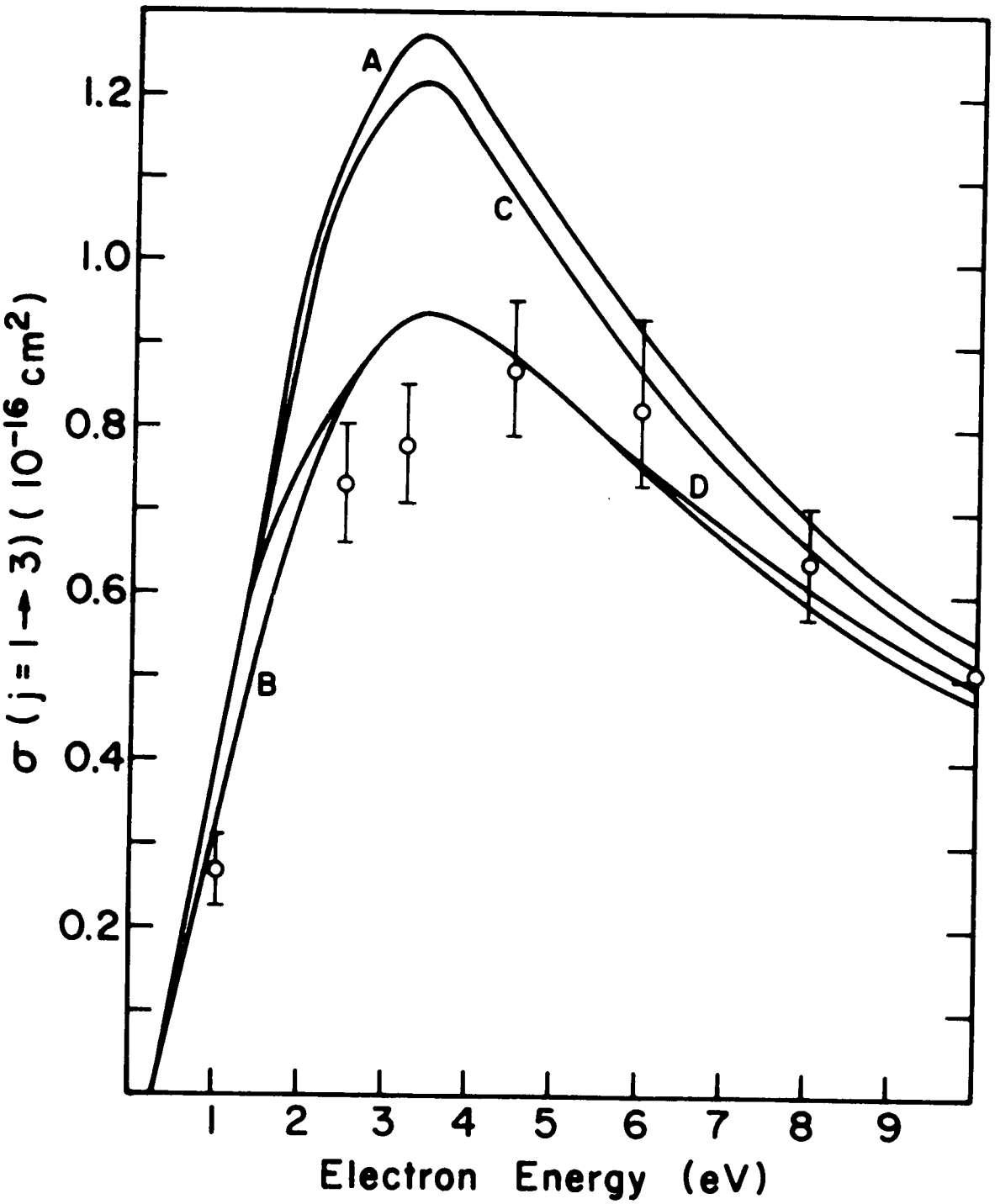
A
B
C
D
1.2
1.0
0.8
0.6
0.4
0.2
σ (j=1→3) (10⁻¹⁶ cm²)
1
2
3
4
5
6
7
8
9
Electron Energy (eV)

Figure 9

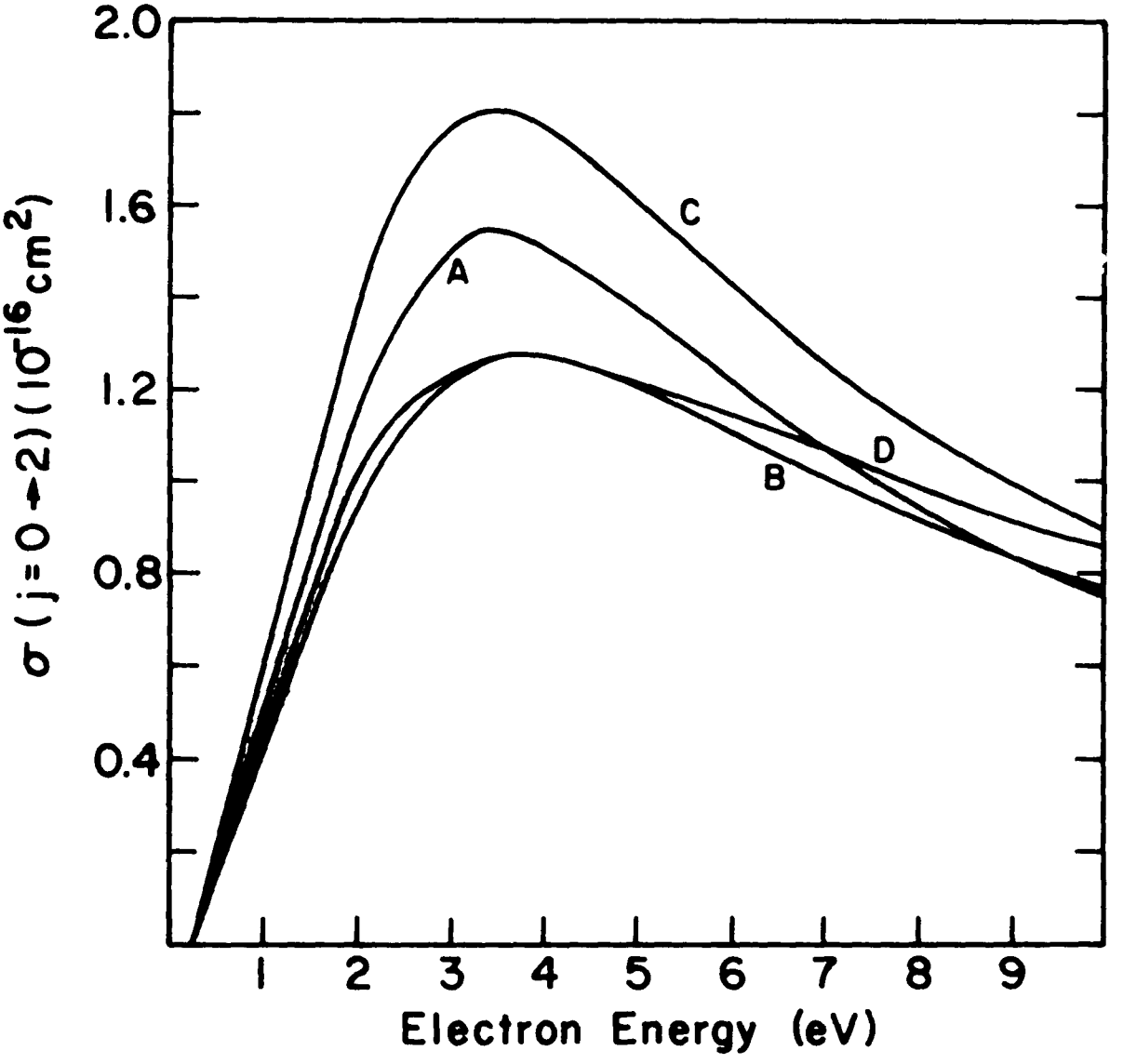
2.0
1.6
1.2
0.8
0.4
σ (j=0→2) (10^16 cm^2)
A
B
C
D
1
2
3
4
5
6
7
8
9
Electron Energy (eV)

Figure 10

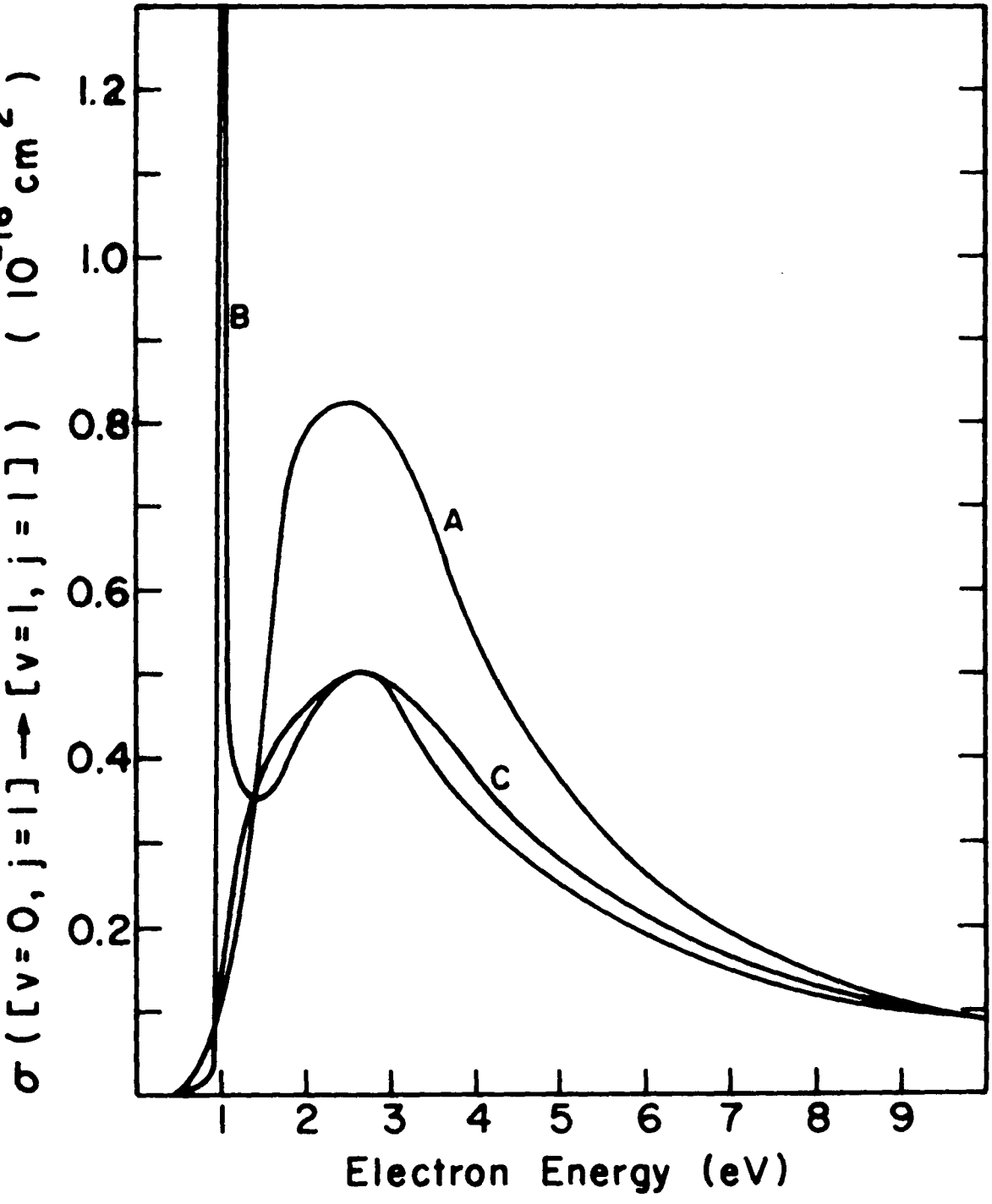
σ ([v=0, j=1] → [v=1, j=1]) (10^{-16} cm^2)
1.2
1.0
0.8
0.6
0.4
0.2
B
A
C
1
2
3
4
5
6
7
8
9
Electron Energy (eV)

Figure 11

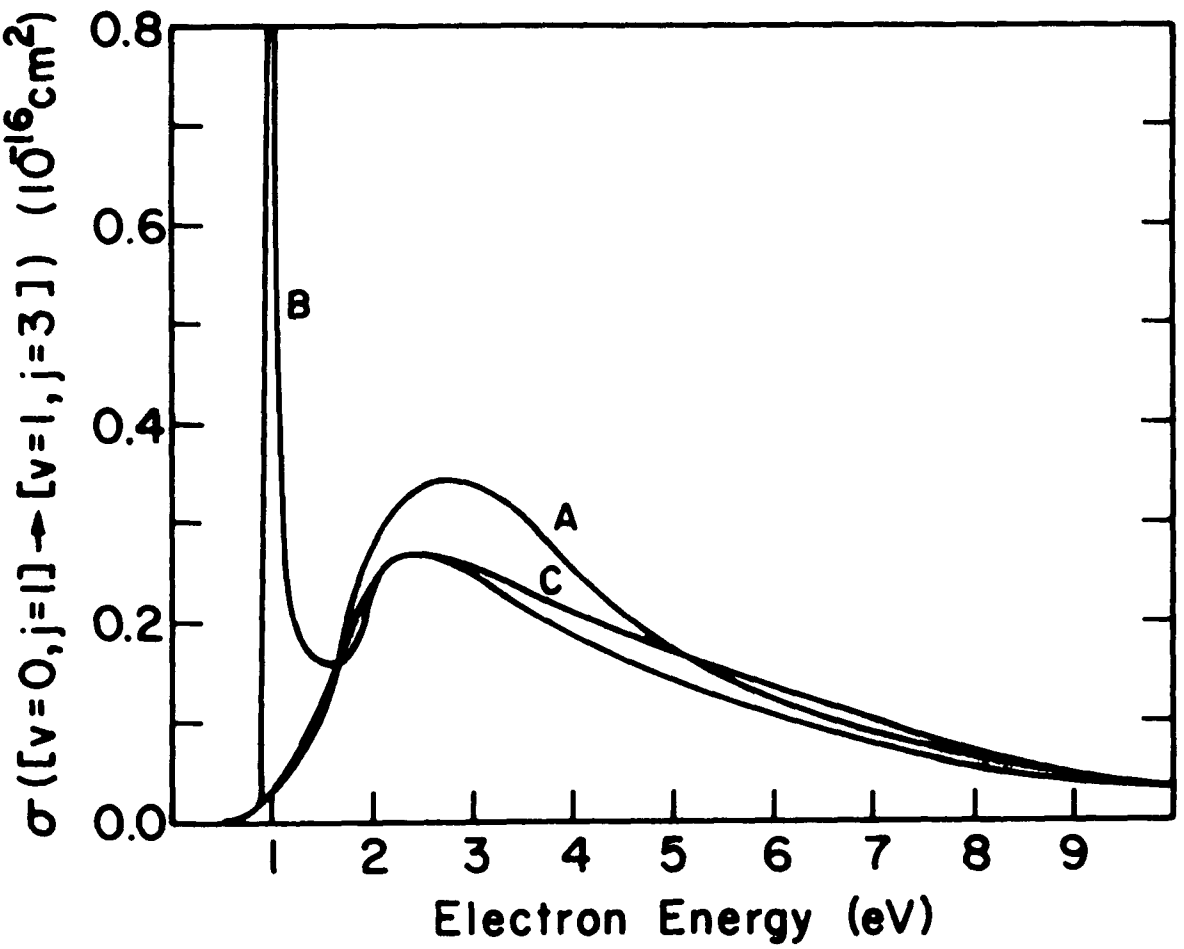
σ([v=0,j=1]→[v=1,j=3]) (10^-16 cm^2)
0.0
0.2
0.4
0.6
0.8
1
2
3
4
5
6
7
8
9
Electron Energy (eV)
A
B
C

Figure 12

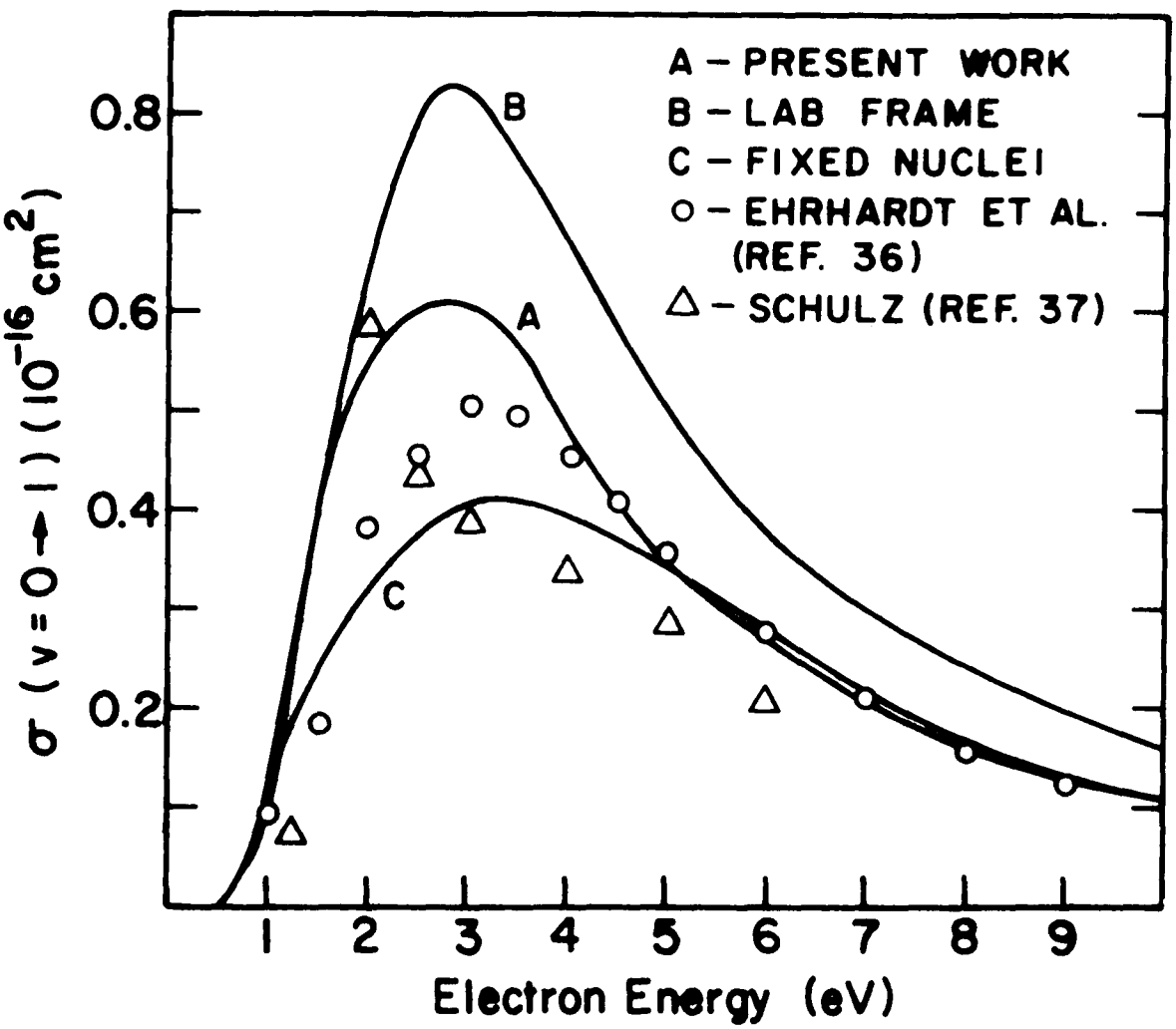
A – PRESENT WORK
B – LAB FRAME
C – FIXED NUCLEI
o – EHRHARDT ET AL. (REF. 36)
Δ – SCHULZ (REF. 37)
σ (v=0→1) (10⁻¹⁶ cm²)
0.8
0.6
0.4
0.2
A
B
C
1
2
3
4
5
6
7
8
9
Electron Energy (eV)

Figure 13

TABLE 1

Long-Range Potential Parameters

Averaged Over Vibrational States

v_i	v_j	$(e\, a_o^2)$ $\langle v_i \lvert Q \rvert v_j \rangle$	(a_o^3) $\langle v_i \lvert \alpha_o \rvert v_j \rangle$	(a_o^3) $\langle v_i \lvert \alpha_2 \rvert v_j \rangle$
0	0	0.484	5.414	1.349
0	1	-0.088	-0.739	-0.406
1	1	0.536	5.885	1.658
0	2	-0.011	-0.071	-0.0075
1	2	-0.123	-1.070	-0.623
2	2	0.586	6.373	1.995

TABLE 2

$\sigma(j=1\rightarrow 3)\ (10^{-16}cm^2)$

Energy (eV) \ $r_t(a_o)$	0.0	1.5	3.5	7.0	15.0	F.T. Result
1.0	.387	.315	.355	.403	.406	.38
2.0	.972	.714	.851	.960	.959	.76
3.0	1.237	.914	1.126	1.199	1.195	.91
4.0	1.203	.919	1.145	1.154	1.153	.92
5.0	1.067	.844	1.046	1.019	1.019	.84
6.0	.923	.752	.920	.878	.880	.76
7.0	.797	.666	.800	.758	.760	.68
8.0	.693	.592	.697	.661	.661	.61
9.0	.609	.529	.611	.581	.581	.54
10.0	.541	.477	.539	.516	.515	.49

TABLE 3

$\sigma(j=0\rightarrow2)\,(10^{-16}cm^2)$

Energy (eV) \ $r_t(a_o)$	0.0	1.5	3.5	7.0	15.0	F.T. Result
1.0	.505	.432	.508	.602	.622	.50
2.0	1.171	.937	1.188	1.389	1.394	1.02
3.0	1.504	1.223	1.629	1.778	1.774	1.23
4.0	1.508	1.276	1.736	1.774	1.774	1.73
5.0	1.376	1.215	1.653	1.616	1.619	1.22
6.0	1.218	1.116	1.501	1.430	1.434	1.14
7.0	1.072	1.013	1.338	1.259	1.263	1.07
8.0	.946	.920	1.187	1.113	1.116	.99
9.0	.842	.837	1.055	.991	.993	.91
10.0	.755	.761	.942	.889	.890	.86

TABLE 4

$\sigma([v=0,j=1]\rightarrow[v=1,j=1])\ (10^{-16}cm^2)$

Energy (eV) \ $r_t(a_o)$	0.0	0.5	1.2	1.7	5.0	F.T. Result
1.0	.147	.147	.691	.854	.451	.15
2.0	.797	.771	.646	.617	.948	.46
3.0	.794	.778	.601	.563	.773	.49
4.0	.557	.553	.444	.426	.522	.38
5.0	.382	.383	.321	.317	.353	.28
6.0	.270	.273	.237	.239	.241	.21
7.0	.199	.203	.180	.185	.180	.16
8.0	.152	.155	.141	.147	.139	.13
9.0	.119	.122	.112	.118	.110	.11
10.0	.095	.098	.091	.097	.091	.09

TABLE 5

$\sigma([v=0,j=1]\rightarrow[v=1,j=3])\ (10^{-16}cm^2)$

Energy (eV) \ $r_t(a_o)$	0.0	0.5	1.2	1.7	5.0	F.T. Result
1.0	.033	.035	.561	.789	.178	.03
2.0	.280	.278	.345	.368	.406	.23
3.0	.335	.332	.318	.321	.357	.26
4.0	.253	.251	.227	.228	.252	.21
5.0	.176	.175	.157	.158	.173	.17
6.0	.123	.123	.110	.112	.121	.12
7.0	.089	.089	.079	.082	.088	.09
8.0	.066	.066	.059	.062	.065	.07
9.0	.050	.051	.045	.047	.050	.05
10.0	.039	.040	.036	.030	.039	.04

TABLE 6

$\sigma([v=0,j=0] \rightarrow [v=1,j=0])\ (10^{-16} cm^2)$

Energy (eV) \ $r_t (a_o)$	0.0	0.5	1.2	1.7	5.0	F.T. Result
1.0	.031	.032	.101	.142	.150	.03
2.0	.151	.151	.184	.212	.325	.16
3.0	.172	.171	.189	.214	.300	.20
4.0	.134	.134	.148	.170	.223	.18
5.0	.100	.100	.112	.130	.161	.16
6.0	.075	.075	.085	.099	.120	.12
7.0	.058	.059	.066	.078	.091	.09
8.0	.046	.046	.052	.062	.072	.07
9.0	.037	.037	.042	.050	.058	.06
10.0	.030	.031	.034	.041	.047	.05

TABLE 7

$\sigma([v=0,j=2]\rightarrow[v=1,j=2])\ (10^{-16}cm^2)$

Energy (eV) \ $r_t(a_o)$	0.0	0.5	1.2	1.7	5.0	F.T. Result
1.0	.031	.031	.104	.132	.098	.03
2.0	.194	.193	.191	.184	.209	.19
3.0	.234	.237	.200	.184	.196	.20
4.0	.189	.187	.155	.141	.146	.14
5.0	.137	.137	.113	.104	.105	.11
6.0	.099	.100	.082	.076	.077	.08
7.0	.074	.075	.062	.058	.057	.06
8.0	.056	.058	.048	.044	.045	.04
9.0	.044	.045	.038	.035	.035	.03
10.0	.035	.036	.030	.028	.028	.02

TABLE 8

$\sigma([v=0,j=0]\rightarrow[v=1,j=2])\,(10^{-16}\,cm^2)$

Energy (eV) \ $r_t(a_o)$	0.0	0.5	1.2	1.7	5.0	F.T. Result
1.0	.034	.035	.156	.223	.169	.03
2.0	.243	.241	.277	.301	.414	.25
3.0	.316	.313	.305	.317	.412	.30
4.0	.258	.252	.241	.252	.315	.28
5.0	.188	.188	.178	.188	.228	.23
6.0	.137	.137	.130	.140	.166	.17
7.0	.101	.102	.097	.104	.124	.12
8.0	.077	.078	.075	.082	.095	.09
9.0	.060	.061	.058	.065	.074	.07
10.0	.047	.048	.048	.052	.059	.05

APPENDIX A

POLARIZATION POTENTIAL

In order to compensate for truncation of the close-coupling expansion to the ground electronic state, an effective polarization potential must be included. Lane and Henry[9] did this by using a trial wave function, in a Rayleigh-Ritz procedure, of the form

$$\psi_{xz} = \phi_o(\vec{r}_1,\vec{r}_2;s) \sum_{\alpha,\beta} C_{\alpha\beta}(\vec{r},s)(x_1+x_2)^{\alpha}(z_1+z_2)^{\beta} \qquad (A1)$$

The total energy of the static e^--H_2 system is minimized with respect to the parameters $C_{\alpha\beta}$, where ϕ_o is the ground electronic state of H_2. The resulting minimum energy $E_m(r,s)$ then yields the polarization potential

$$V_P(r,s) = E_m(r,s) - E_o(s) - \langle\phi_o|V|\phi_o\rangle \qquad (A2)$$

where $E_o(s)$ is the unperturbed ground state energy and V is the static interaction. This polarization potential is the one used in the present paper.

One is tempted to improve on this polarization potential by employing a trial wave function of the form

$$\psi_{xzr} = \phi_o(\vec{r}_1,\vec{r}_2;s) \sum_{\alpha\beta\gamma} C_{\alpha\beta\gamma}(\vec{r},s)(x_1+x_2)^{\alpha}(z_1+z_2)^{\beta}$$

$$(r_1+r_2)^{\gamma} \qquad \text{(A3)}$$

It was found however,[23] that such an inclusion of variations in r_1 and r_2 amount to non-dipole contributions to the polarization potential. Obedkov[24] has shown that only dipole effects should be included in a polarization calculation in the context of the adiabatic approximation.

Figure 5 shows a comparison with a calculation of Hara[25] in which he, through a perturbation treatment, explicitly puts in only dipole contributions. Curve A shows the resulting variational polarization potential when one includes only X, Z variations. Curve B shows the results of including X, Z, r contributions. Curve B of Figure 6 shows the overestimation of the total vibrational cross section that results from including X, Z, r variations. The ground state H_2 electronic wave function used is that of Browne.[26]

APPENDIX B

GREEN'S FUNCTIONS

Coordinate space Green's functions are required by the NIIEM method for application to neutral and charged systems. These functions are solutions to the equation

$$\frac{d^2}{dr^2} y_\ell^{(\frac{1}{2})}(r) + \left[\pm(|k|)^2 + \frac{2(Z-N)}{r} - \frac{\ell(\ell+1)}{r^2}\right] y_\ell^{(\frac{1}{2})}(r) = 0 \tag{B1}$$

where Z is the nuclear charge, N is the negative charge, $K = |k|^2$ is the magnitude of the energy, ℓ is the angular momentum, $(\pm)$ indicates $(^{\text{open}}_{\text{closed}})$ channels, $y_\ell^{(1)}(r)$ is the solution regular at the origin, and $y_\ell^{(2)}(r)$ is the solution irregular at the origin. The functions $y_\ell^{(1)}$ and $y_\ell^{(2)}$ must be linearly independent for all r. This is insured by requiring that they satisfy the Wronskian relation

$$\left[\frac{d}{dr} y_\ell^{(1)}(r)\right] y_\ell^{(2)}(r) - y_\ell^{(1)}(r) \left[\frac{d}{dr} y_\ell^{(2)}(r)\right] = 1 \tag{B2}$$

The open channel boundary conditions are given by

$$y_\ell^{(1)}(r) = F_\ell(r) \begin{cases} \underset{r\to 0}{\sim} r^{\ell+1} \\ \underset{r\to\infty}{\sim} \frac{1}{k^{1/2}} \sin[|<r - \eta \ell n(2|<r) - \frac{\ell\pi}{2} + \sigma_\ell] \end{cases}$$

$$y_\ell^{(2)}(r) = G_\ell(r) \begin{cases} \underset{r\to 0}{\sim} \frac{1}{r^\ell} \\ \underset{r\to\infty}{\sim} \frac{1}{k^{1/2}} \cos[|<r - \eta \ell n(2|<r) - \frac{\ell\pi}{2} + \sigma_\ell] \end{cases} \qquad \text{(B3)}$$

where

$$\sigma_\ell = \arg \Gamma(\ell+1+i\eta) = |\Gamma(\ell+1+i\eta)\, e^{i\sigma_\ell}$$

$$\eta = -(Z-N)/K \qquad \text{(B4)}$$

It's useful to define an alternative integration variable $\rho = Kr$. Thus (B1) becomes

$$\frac{d}{d\rho^2} y_\ell(\rho) + [1 - \frac{2\eta}{\rho} - \frac{\ell(\ell+1)}{\rho^2}]\, y_\ell(\rho) = 0 \qquad \text{(B5)}$$

The boundary conditions are then

$$f_\ell(\eta,\rho) \begin{cases} \underset{\rho\to 0}{\sim} \rho^{\ell+1} \\ \underset{\rho\to\infty}{\sim} \sin[\rho - \eta \ell n 2\rho - \frac{\ell\pi}{2} + \sigma_\ell] \end{cases}$$

$$g_\ell(\eta,\rho) \begin{cases} \rho\to 0 \quad 1/\rho\ell \\ \underset{\rho\to\infty}{\sim} \cos[\rho - \eta \ell n\, 2\rho - \frac{\ell\pi}{2} + \sigma_\ell] \end{cases} \qquad \text{(B6)}$$

where we now require

$$(\frac{d}{d\rho} f_\ell) g_\ell - f_\ell (\frac{d}{d\rho} g_\ell) = 1 \qquad \text{(B7)}$$

Thus

$$F_\ell(r) = \frac{1}{\sqrt{K}} f_\ell$$

$$G_\ell(r) = \frac{1}{\sqrt{K}} g_\ell \qquad \text{(B8)}$$

We note a useful check on the calculated functional values

$$[f_{\ell-1} g_\ell - f_\ell g_{\ell-1}] \; / \; [\ell/(\ell^2+\eta^2)^{1/2}] = 1 \qquad \text{(B9)}$$

We may define[28] an auxillary function by

$$f_\ell = C_\ell(\eta) \rho^{\ell+1} \Phi_\ell(\eta,\rho)$$

$$\Phi_\ell(\eta,\rho) = \sum_{n=\ell+1}^{\infty} A_n^\ell(\eta) \rho^{n-\ell-1} \qquad \text{(B10)}$$

where

$$A_{\ell+1}^\ell = 1$$

$$A_{\ell+2}^\ell = \eta/(\ell+1)$$

$$(n+\ell)(\eta-\ell-1) A_n^\ell = 2\eta \, A_{n-1}^\ell - A_{n-2}^\ell \; ; \; n>\ell+2 \qquad \text{(B11)}$$

Also

$$C_\ell^2(\eta) = \frac{P_\ell(\eta)C_o^2(\eta)}{2\eta(2\ell+1)}$$

$$C_\ell = \frac{(\ell^2+\eta^2)^{1/2}}{\ell(2\ell+1)} C_{\ell-1}$$

$$C_o^2 = 2\pi\eta/(e^{2\pi\eta}-1)$$

$$P_\ell(\eta)/2\eta = \frac{1(1+\eta^2)(4+\eta^2)\ldots(\ell^2+\eta^2)2^{2\ell}}{(2\ell+1)[(2\ell)!]^2} \qquad \text{(B12)}$$

The irregular solution is given by

$$g_\ell = \frac{2\eta}{C_o^2} f_\ell \left[\ell n\, 2\rho + \frac{q_\ell(\eta)}{P_\ell(\eta)}\right] + \theta_\ell(\eta,\rho) \qquad \text{(B13)}$$

where

$$\theta_\ell(\eta,\rho) = D_\ell(\eta)\frac{1}{\rho^\ell}\psi_\ell(\eta,\rho)$$

$$D_\ell(\eta)C_\ell(\eta) = 1/(2\ell+1)$$

$$\psi_\ell(\eta,\rho) = \sum_{n=-\ell}^{\infty} a_n^\ell(\eta)\rho^{n+\ell} \qquad \text{(B14)}$$

also

$$a^{\ell}_{-\ell} = 1$$

$$a^{\ell}_{-\ell+1} = 0$$

$$(n-\ell-1)(n+\ell)a^{\ell}_{n} = 2\eta\ a^{\ell}_{n-1} - a^{\ell}_{n-2} \ ;\ n = -\ell,-\ell+1,\ldots,\ell$$

$$(n-\ell-1)(n+\ell)a^{\ell}_{n} = 2\eta\ a^{\ell}_{n-1} - a^{\ell}_{n-2} - (2n-1)P_{\ell}(\eta)A^{\ell}_{n} \ ;$$

$$n = \ell+1,\ldots$$

(B15)

$$\frac{q_{\ell}(\eta)}{P_{\ell}(\eta)} = \sum_{s=1}^{\ell} \frac{s}{s^2+\eta^2} - \sum_{s=1}^{2\ell+1} \frac{1}{s} + R_e\left[\frac{\Gamma'(1+i\eta)}{\Gamma(1+i\eta)}\right] + 2C + \frac{r_{\ell}(\eta)}{P_{\ell}(\eta)} \qquad \text{(B16)}$$

$$r_{\ell}(\eta) = \frac{(-1)^{\ell+1}}{(2\ell)!}\ \mathrm{Im}\left[\frac{1}{2\ell+1} + \frac{2(i\eta-\ell)}{(2\ell)(1!)} + \frac{2^2(i\eta-\ell)(i\eta-\ell+1)}{(2\ell-1)(2!)} + \ldots + \frac{2^{2\ell}(i\eta-\ell)(i\eta-\ell+1)\ldots(i\eta+\ell-1)}{(2\ell)!}\right]$$

$$\mathrm{Re}\left[\frac{\Gamma^1(1+i)}{\Gamma(1+i)}\right] + 2C = 1 + C - \frac{1}{1+\eta^2} + \eta^2 \sum_{k=2}^{\infty} \frac{1}{k(k^2+\eta^2)}$$

$$C = 0.5772156649 \qquad \text{(B17)}$$

$$|\Gamma(\ell+1+i\eta) = [\eta^2(1+\eta^2)(2^2+\eta^2)\ldots(\ell^2+\eta^2)]^{1/2}|\Gamma(i\eta)|$$

$$|\Gamma(i\eta)| = [\pi/(\eta \sinh \pi\eta)]^{1/2}$$

$$|\Gamma(\ell+1+i\eta)| = |\Gamma(\ell+1-i\eta)| \qquad \text{(B18)}$$

For the open channel solutions, the method of computation is to start both the regular and irregular solutions at the origin using (B10) and (B13) respectively, and then integrate using a three point Numerov algorithm with a local truncation error of $h^6 y^{(y)}$, where h is the integration mesh step size. The closed channel boundary conditions are given by

$$y_\ell^{(1)}(r) = F_\ell(r) \begin{cases} \underset{r\to 0}{\sim} & r^{\ell+1} \\ \underset{r\to\infty}{\sim} & e^{Kr+\eta \ell n\ 2Kr} \end{cases}$$

$$y_\ell^{(2)}(r) = G_\ell(r) \begin{cases} \underset{r\to 0}{\sim} & 1/r^{\ell} \\ \underset{r\to\infty}{\sim} & e^{-Kr-\eta\ \ell n\ 2Kr} \end{cases} \qquad \text{(B19)}$$

Thus from (B1) with $\rho=Kr$ we get

$$\frac{d^2}{d\rho^2} y_\ell(\rho) + \left[-1 - \frac{2\eta}{\rho} - \frac{\ell(\ell+1)}{\rho^2}\right] y_\ell(\rho) = 0 \qquad \text{(B20)}$$

We make the substitution

$$m = \ell + \frac{1}{2}$$

$$x = 2\rho = 2Kr$$

$$u = -\eta = \frac{Z-N}{K} \qquad \text{(B21)}$$

and obtain a form of Whittaker's equation

$$\frac{d^2}{dx^2}\,\omega(x) + \left[-\frac{1}{4} + \frac{u}{x} + \frac{\frac{1}{4} - m^2}{x^2}\right]\omega(x) = 0$$

$$; \; 2m = 2\ell+1 = \{1,3,5,\ldots\} \qquad \text{(B22)}$$

We require that the solutions satisfy

$$\omega_F \begin{cases} \underset{x\to 0}{\sim} x^{m+\frac{1}{2}} = (2Kr)^{\ell+1} \\ \underset{x\to\infty}{\sim} \exp\left[\frac{x}{2} - u\ \ell n\ x\right] = \exp(Kr)(2Kr)^{\eta} \end{cases}$$

$$\omega_G \begin{cases} \underset{x\to 0}{\sim} x^{-m+\frac{1}{2}} = (2Kr)^{-\ell} \\ \underset{x\to\infty}{\sim} \exp\left[-\frac{x}{2} + u\ \ell n\ x\right] = \exp[-Kr](2Kr)^{-\eta} \end{cases}$$

(B23)

and

$$\left[\frac{d}{dx}\,\omega_F(x)\right]\omega_G(x) - \omega_F(x)\left[\frac{d}{dx}\,\omega_G(x)\right] = 1 \qquad \text{(B24)}$$

Thus

$$F_\ell(r) = \frac{1}{(2Kr)^{1/2}}\,\omega_F$$

$$G_\ell(r) = \frac{1}{(2Kr)^{1/2}}\,\omega_G \qquad \text{(B25)}$$

We find from Whittaker and Watson,[29] Chapter 16, that our solutions correspond to well-known functions

$$\omega_F(x) = M_{u,m}(x) = x^{m+\frac{1}{2}}\, e^{-\frac{1}{2}x}\; {}_1F_1\left[-\left(u-m-\tfrac{1}{2}\right), 1+2m; x\right]$$

$$\omega_G(x) = W_{u,m}(x) \qquad \text{(B26)}$$

However, we are only interested in positive odd integer values of 2m. Whittaker and Watson do not consider this case and it presents some difficulty, especially in determining values of $W_{u,m}(x)$. For small values of the argument we obtain

$$M_{u,m}(x) \underset{x\to 0}{\sim} x^{m+\frac{1}{2}}\, e^{-\frac{1}{2}x} \left[\frac{(2m)!}{\Gamma[-(u-m-\frac{1}{2})]}\right] \sum_{\nu=0}^{\infty} \frac{\Gamma[-(u-m-\frac{1}{2})+\nu]}{(2m+\nu)!}\,\frac{x\nu}{\nu!} \qquad \text{(B27)}$$

and

$$W_{u,m}(x) \underset{x\to 0}{\sim} \frac{(-1)^{2m} x^{m+\frac{1}{2}} e^{-\frac{1}{2}x}}{\Gamma[-(u+m-\frac{1}{2})]\Gamma[-(u-m-\frac{1}{2})]}\{\sum_{\nu=0}^{\infty} \frac{\Gamma[-(u-m-\frac{1}{2})+\nu]}{(2m+\nu)!}\frac{Z^{\nu}}{\nu!}$$

$$* \ [\psi(\nu+1)+\psi(2m+1+\nu)-\psi[-(u-m-\tfrac{1}{2})+\nu]-\ell n\ Z]$$

$$+ \ (-Z)^{-2m} \sum_{\nu=0}^{2m-1} \Gamma(2m-\nu)\Gamma[-(u+m-\tfrac{1}{2})+\nu] \ \frac{(-Z)^{\nu}}{\nu!}$$

(B28)

where

$$\psi(s) = \Gamma'(s)/\Gamma(s) = -\gamma + \sum_{\nu=1}^{\infty} [\frac{1}{\nu} - \frac{1}{(s+\nu-1)}]$$

$$\psi(n+1) = \psi(n) + \frac{1}{n} \qquad \text{(B29)}$$

The bracketed term in (B27) is divided out for normalization purposes. For large values of the argument

$$W_{u,m}(x) \underset{x\to\infty}{\sim} e^{-\frac{x}{2}} x^{u} [1 + \sum_{\nu=1}^{\infty} \frac{1}{\nu! x^{\nu}}$$

$$[m^2-(u-\tfrac{1}{2})^2][m^2-(u-\tfrac{3}{2})^2]\ldots[m^2-(u-\nu+\tfrac{1}{2})^2]]$$

(B30)

and

$$M_{u,m}(x) \underset{x\to\infty}{\sim} \left[\frac{\Gamma(1+2m)}{\Gamma[-(u-m-\frac{1}{2})]} \right] e^{\frac{1}{2}x}\, x^{-u}$$

$$\left[1 + \sum_{\nu=1}^{\infty} \frac{1}{\nu! x^{\nu}} \left[(u+\tfrac{1}{2})^2 - m2\right]\right.$$

$$\left. * \left[(u+\frac{3}{2})^2 - m^2\right] \ldots \left[(u+\nu-\tfrac{1}{2})^2 - m^2\right] \right. \qquad \text{(B31)}$$

where the first bracketed term in $M_{u,m}(x)$ is again divided out for normalization purposes. $M_{u,m}(x)$ is generated using (B27) for small X. It is then integrated outward using a three point Numerov algorithm with a local truncation error of $h^6 y^{(y)}$. This technique is also applied at infinity to $W_{u,m}(x)$ using Eq. (B30).

VITA

Charles Albert Weatherford was born in Mobile, Alabama on June 23, 1947. He graduated from Baker High School, Baker, Louisiana in 1965. He received his B.S. in physics from Louisiana State University in 1969.

EXAMINATION AND THESIS REPORT

Candidate: WEATHERFORD, Charles Albert

Major Field: Physics

Title of Thesis: Frame Transformations in Electron-Molecule Scattering

Approved:

Ronald g. Henry
Major Professor and Chairman

James D. Ivory
Dean of the Graduate School

EXAMINING COMMITTEE:

John Kimball

G. H. Fe Canini

R. F. O' Connell

Arlo U. Landolt

Date of Examination:

July 19th, 1974